Counterion Condensation, the Gibbs Equation, and Surfactant Binding: an Integrated Description of the Behaviour of Polyelectrolytes and their Mixtures with Surfactants at the Air–Water Interface

Jeffrey Penfold[†] and Robert K.Thomas[*,‡]

†*STFC, Rutherford-Appleton Laboratory, Chilton, Didcot, Oxfordshire, OX11 0RA, United Kingdom*

‡*Physical and Theoretical Chemistry Laboratory, South Parks Road, Oxford, OX1 3QZ, United Kingdom*

E-mail: robert.thomas@chem.ox.ac.uk

Abstract

By applying the Gibbs equation to the bulk binding isotherms and surface composition of the air-water (A-W) interface in polyelectrolyte-surfactant (PE-S) systems, we show that their surface behaviour can be explained semiquantitatively in terms of four concentration regions, which we label A, B, C and D. In the lowest concentration range A there are no bound PE-S complexes in the bulk but there may be adsorption of PE-S complexes at the surface. When significant adsorption occurs in this region the surface tension (ST) drops with increasing concentration like a simple surfactant solution. Region B extends from the onset of bulk PE-S binding to the end of cooperative binding, in which the slow variation of surfactant activity with cooperative binding means that the ST changes relatively little, although adsorption may be significant. This leads to an approximate plateau, which may be at high or low ST. Region C starts where the binding in the bulk complex loses its cooperativity leading to a rapid change of surfactant activity with total concentration. This, combined with significant adsorption often leads to a sharp drop in ST. Region D is where precipitation and redissolution of the bulk PE-S complex occurs. ST peaks may arise in region D because of loss of the solution complex that matches the value of the preferred surface stoichiometry, which seems to have a well defined value for each system. The analysis is applied to the experimental systems, sodium polystyrene sulfonate-alkyltrimethylammonium bromides and poly(diallyldimethyl chloride)-sodium alkyl sulfates, with and without added electrolyte, and includes data from bulk binding isotherms, phase diagrams, aggregation behaviour, and direct measurements of the surface excess and stoichiometry of the surface. The successful fits of the Gibbs equation to the data confirm that the surfaces in these systems are largely equilibrated.

Introduction

Oppositely charged polyelectrolyte–surfactant (PE–S) mixtures are widely used in formulations because they are used to enhance surface activities and adjust rheological properties of

solutions. Their behaviour at the air–water (A-W) interface is a particular target for research because it can be defined by the thermodynamic property of surface tension (ST), which can then be used as a starting point for explaining properties such as wetting and spreading, which determine the operational properties of such mixtures. Goddard[1,2] and Thompson[3] have written important early reviews on these issues. There are many later reviews of PE-S complexes in solution, several of which explicitly consider interfacial behaviour.[4–11]

The majority of experimental measurements on PE-S mixtures at the A-W interface follow the surface behaviour of a fixed and relatively dilute PE concentration of 10-1000 ppm (or 0.05-5 mM monomer) as a function of added surfactant. The ST of the mixture is generally lower than for the surfactant alone and it has several distinctive features which have led to PE-S mixtures being divided empirically into two groups.[5] In Type 1 the initial fall in ST depends on the starting concentration of polymer, the mixture exhibits no sharp peak in the ST at or close to precipitation, and there is a tendency of the system to form multilayers at higher concentrations. Multilayering in PE-S systems most commonly means that a bilayer adsorbs underneath the usual monolayer at the A-W interface and such layers are readily identified by neutron reflection (NR).[11,12] An example of Type 1 behaviour is sodium polystyrene sulfonate (PSS)-dodecyltrimethylammonium bromide (C_{12}TAB). In Type 2 behaviour, the initial drop in ST does not depend on the PE concentration, there is often a peak in the ST close to precipitation, and no multilayering is observed at any concentration. A system that follows Type 2 behaviour is poly(diallyldimethylammonium chloride) (PDDA)-sodium dodecyl sulfate (SDS).

We have shown using either mass action[13,14] or thermodynamic arguments[15] that it is possible to account for several ST features of Type 1 and Type 2 systems. The binding isotherms that characterize the formation of PE-S complexes in bulk solution have also been extensively studied,[16,17] but a puzzling feature of the surface behaviour has been that the onset of ST lowering mostly seems to occur at concentrations much higher than those at which PE-S complexes form in the bulk solution,[18] although the Gibbs equation requires a close

connection between binding isotherm and surface behaviour. A proposal that the binding constant of a PE-S complex is proportional to the product of 1/CMC of the surfactant and the squared linear charge density of the polyelectrolyte[19] further suggests a connection between surface behaviour and the linear charge density of the polyelectrolyte. We have recently established links between bulk complex formation and the ST that suggest that some of the features identified in the two PE-S systems above may be connected with cooperativity in the binding curve.[20] However, those links were incomplete and the surface behaviour was significantly dependent on assumptions about the solution structures of the complexes, which is information that is often not available from experiment. We now extend that exploration to a fuller study of the effects of the strength and form of the binding on the surface behaviour using more general considerations and making use of the surface composition, which can be determined experimentally.

The electrostatic interaction of counterions with a polyelectrolyte leads to the phenomenon of counterion condensation, which has a large effect on the thermodynamic properties of the polyelectrolyte[21–24] and hence on the ST via the Gibbs equation.[22,25,26] Any dependence of the surfactant binding on the axial charge density would then suggest that the thermodynamic consequences of surfactant binding and counterion condensation have some parallels. The thermodynamics of counterion condensation is relatively well understood at a theoretical level and it may therefore throw some light on the thermodynamics of surfactant binding, particularly as it relates to the A-W interface. As well as interacting cooperatively, counterions and surfactant ions may compete or at least interfere with each other, with further consequences for the properties of PE-S complexes. In this paper we examine the effect of this balance on the PE-S binding curves and on the surfaces of both polyelectrolytes and PE-S mixtures.

An experimental difficulty in studying the surface of PE-S mixtures is that bulk and surface processes involving polymers become slower as the molecular weight (MW) increases and this is particularly the case when there is also precipitation. It is always difficult to

establish experimentally whether surface equilibrium has truly been reached. Formally, it can only be done by showing that the Gibbs equation is obeyed for a given system. It is, however, rarely possible to apply the Gibbs equation quantitatively to any PE-S system. Although our previous analyses have used the Gibbs equation,[15] these analyses require a level of empirical input, and this is not the same as demonstrating that the Gibbs equation is fully obeyed. A subsidiary aim of this paper is therefore to extend the analysis to allow the various patterns of surface behaviour to be accounted for qualitatively, or preferably semiquantitatively, in terms of the Gibbs equation, and thereby to help to establish whether or not they are equilibrium phenomena.

Polyelectrolyte Adsorption and the Gibbs Equation

The adsorption of polyelectrolytes at the A-W interface is experimentally not well characterized and the application of the Gibbs equation is made uncertain because of the large contribution of counterions to the ST behaviour. For a polyelectrolyte, P, bound to ν univalent counterions, Y, the Gibbs equation can be written in terms of the mean activity of the polyelectrolyte as[27]

$$d\sigma = -(\nu+1)\Gamma_P RTd\ln a_\pm = -(\nu+1)\Gamma_P RTd\ln c_\pm f_\pm \tag{1}$$

where Γ_P is the total molar surface excess of polymer in whatever form, and the mean activity $a_\pm$ is given by

$$a_\pm = \left[a_P a_Y^\nu\right]^{\frac{1}{\nu+1}} \tag{2}$$

with similar expressions holding for the mean concentration, $c_\pm$, and mean activity coefficient, $f_\pm$. In the absence of other ions, Eqn (1) can then be written in terms of either the counterion, Y, or the polymer monomer, X, as

$$d\sigma = -\Gamma_X RTd\ln c_X f_\pm \approx -\Gamma_X RTd\ln c_X \tag{3}$$

where $(\nu + 1)/\nu$ has been approximated to 1, and c_X has been taken to be equal to $c_\pm$, substitutions that are accurate except at low MW. The right hand side of Eqn (3) assumes complete dissociation and ideal behaviour, neither of which is appropriate for most polyelectrolyte systems. However, this limit illustrates the requirement that a large number of counterions have to be adsorbed per polyion to maintain neutrality, and their loss of entropy may then become the factor dominating changes in the ST. Thus, for a typical monomer surface excess at the A-W interface the slope of the resultant ideal Gibbs plot would be comparable ith that for a surfactant. However, the counterions of polyelectrolytes are often extensively condensed on to the polyion in solution and are therefore far from ideal. The correct application of the Gibbs equation to polyelectrolytes[26] therefore requires a determination of $f_\pm$ of the polyelectrolyte.

Counterion condensation occurs when the separation of charge along the axis of the polyelectrolyte is less than the Bjerrum length, l_b, which is the distance at which the electrostatic repulsion between identically charged monovalent ions in water is equal to k_BT ($l_b \approx 7$ Å). If the axial separation of charge on the polyion, l, is shorter than l_b, ions from the surroundings condense on the rod to relieve the electrostatic stress in the system.[21,22] The fractional degree of ionization of the polyelectrolyte can be defined in terms of the parameter ξ, which is given by

$$\xi = \frac{q^2}{\epsilon k_B T l} = \frac{l_b}{l} \tag{4}$$

where ϵ is the bulk dielectric constant of water. Combining this with the Debye-Huckel theory gives the result that counterion condensation occurs on the rod when $\xi > 1$ to give a fractional degree of dissociation, which is $1/\xi$ for a polyelectrolyte with monovalent counterions. This leads to the further result that[28]

$$\ln f_\pm = \left(\frac{1}{2\xi} - 1\right) \ln c_X + \text{constant} \tag{5}$$

and Eqn (3) becomes

$$d\sigma = -\frac{\Gamma_X RT}{2\xi} d\ln c_X \tag{6}$$

For example, the value of ξ is about 4 for double stranded DNA, just under 3 for NaPSS and other vinyl based polyelectrolytes,[19] and close to 2 for PDDA,[29–31] all with monovalent counterions. Thus, DNA, NaPSS and PDDA should be about 25%, 33% and 50% dissociated respectively in the counterion condensed limit. In more elaborate models, which include the local charge separation and dielectric constant, these values may change so that, for example, vinyl polyelectrolytes may have different effective ξ values.[23]

It is convenient to use polystyrene sulfonate (PSS) in a monovalent cation form such as NaPSS to illustrate the problems associated with ST measurements of polyelectrolytes and as a basis for interpreting PE-S behaviour. The use of a strong polyelectrolyte removes the complication of ionization varying with pH, and the A-W surfaces of PSS solutions are the most studied of the strong polyelectrolytes. Many weak polyelectrolytes involve carboxylic acid dissociation and this introduces a further complication over the positioning of the water dividing surface, which requires adjustments to the simple forms of the Gibbs equation given above.[32] The monomer units in polyelectrolytes are amphiphilic, which may cause them to adsorb at the A-W interface. However, because the hydrophobic fragment is generally shorter than a typical surfactant, the aqueous surface is less well screened than for an ionic surfactant and the tendency to adsorb is then relatively weak. The close spacing of segments and the steric restrictions required to align them at the A-W surface further affect adsorption and may cause the adsorption per segment to vary with molecular weight, MW. The activity of polyelectrolytes in bulk solution is also expected to change at the dilute-semidilute crossover, c_r, for which the variation with MW for NaPSS has been given by Nishida et al.[33] The MW dependence of the bulk behaviour of dilute solutions of polyelectrolytes is also affected by electrostatic interactions. Thus, Muthukumar has shown that electrostatic correlations lead to a κ peak in the x-ray or neutron small angle scattering as well as contributing significantly to $f_\pm$[34] in Eqn (3). Experimental measurements of the surface properties of polyelectrolytes

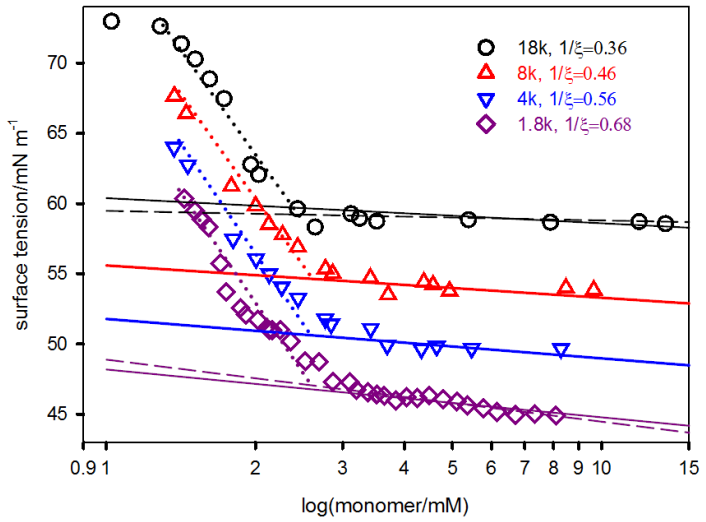

Figure 1: Variation of the ST for a series of PSS polyelectrolytes of different MW as a function of monomer molar concentration. Linear fits are shown for the higher concentration range data, dashed lines are explained in the text, and dotted lines are approximate fits to the low concentration data with identical gradients. The data are redrawn from Caminati and Gabrielli.[36]

are also challenging in that equilibration is slow[35] and the low surface activity makes the ST sensitive to low levels of impurity.

Equilibration should be faster for low MW samples. Caminati and Gabrielli (CG) used such a set of samples of PSS with MW of 1.8k, 4k, 8k and 18k with a moderately low polydispersity. The ST results in Figure 1[36] show significant adsorption at low concentrations (1-10 mM of monomer) for all four MW and CG did not report any difficulty in reaching equilibrium ("measurements were taken for each concentration at 20 min intervals until equilibrium was reached"). The ST decreases with MW and each of the ST plots is concave with respect to the axes, which does not normally occur in a Gibbs plot unless there is some sort of transition in the bulk solution that causes a change in the activity. This was assumed by CG, who therefore fitted the Gibbs equation to the *initial* low concentration slopes of the data in Figure 1. It is, however, difficult to identify any transition that might occur at such low concentrations because the system is an order of magnitude below c_r, which is estimated to be 150 mM for the 18k polymer and higher for lower MW,[33,37] and lower even than c_κ,

which is the concentration at which there is overlap of the ionic atmospheres of the polyelectrolytes, which is estimated to be 12 mM for the 18k polymer.[33,37] We have argued elsewhere that polydispersity in combination with depletion may cause an anomalous steep variation of the ST of polymers at low concentrations.[38] We propose a related mechanism below, which would mean each ST curve can only be analysed quantitatively at concentrations *above* the break in slope.

Interpretation of the data in Figure 1 requires a knowledge of either the fractional charge ($1/\xi$) on the polymer or its mean activity coefficient. There are no mean activity coefficient measurements for such low MW PSS. However, since CG's measurements, Bohme and Scheler have determined $1/\xi$ of PSS over a wide range of MW using NMR electrophoresis.[39,40] The measurements, shown in Figure S1 of the Supplementary Information, show that $1/\xi$ decreases as the MW increases with the lowest MW polymers being nearly completely dissociated. The data can be fitted with the quadratic curve shown in Figure S1, which gives fractional charges of 0.68, 0.56, 0.46 and 0.36 for the MWs of 1.8k, 4.6k, 8k and 18k respectively used by CG. These values with Eqn (6) and a constant Γ_X of 1.7 μmol m^{-2} gave the fits shown in Figure 1 as solid lines. Although there is significant error in the slopes, there is an indication that the data at 1.8k and 18k might be better fitted by the respectively increased and decreased slopes of the dashed lines in Figure 1. Such a change would be consistent with the observed increase in limiting ST with MW. The results overall give a value of Γ_X of 1.7 μmol m^{-2} ($\approx$ 100 Å^2 per segment) which is lower than the typical value for surfactants at saturation (3-4 μmol m^{-2}). In contrast, CG's use of the low concentration slopes gave adsorbed areas per segment of 42, 24, 22 and 17 Å^2 respectively for MWs of 1.8k, 4.6k, 8k and 18k, which would be expected to lead to a MW dependence of ST opposite to that observed.

Effects of polydispersity often couple with depletion effects. Depletion may be an equilibrium effect in that the adsorbing solute is lost to the various surfaces in the system during the set up of an ST experiment, or it may be a kinetic effect in that there is a slow rate

of diffusion to the surface. In a polymer system polydispersity can couple with kinetic depletion in that small MW species equilibrate with the surface more rapidly than large MW. However, the adsorption energy of a large MW species is generally greater so that large MW species in time replace small MW at the surface. This is the case even if, as here, the mean adsorption energy per segment decreases with increasing MW. As the concentration is lowered the time taken for the large MW species will increase rapidly, especially when the typical depletion range of about 10^{-2} mM (*whole polymer*) is reached.[41] There are then two possibilities for depletion in the low concentration part of CG's PSS experiments. Either an apparent equilibrium is reached where smaller MW species occupy the surface initially and their replacement by large species is too slow to be observed in the relatively short timescale of the experiments, or there is significant loss of the higher MW species to the various sample surroundings below a threshold concentration of about 10^{-2} mM of polymer, i.e. the larger MW species do not sustain full adsorption even in the absence of small MW species. Such a mechanism has been used to explain a similar ST pattern in a nonionic polymer[38] where the steeper slope at low concentration was attributed to the smaller area per molecule, i.e. a higher molar coverage in the Gibbs equation.

The use of $1/\xi$ in the analysis above suggests that the ST behaviour might be usefully approached via the bulk counterion binding, partle because bulk aggregation is less sensitive to contaminants or dispersity than the surface. Thus, Eqn (1) can be used to estimate changes in the ST from experimental measurements of the bulk mean activity coefficient, $f_{\pm}$. Measurements of $f_{\pm}$ of polyelectrolytes, however, have a technical limitation that arises from the persistence of counterion condensation down to zero concentration. Unlike a mass action controlled equilibrium, the limiting value of $f_{\pm}$, i.e. f_0, does not approach the normal limit of 1 at infinite dilution, and therefore has to be expressed relative to an arbitrary reference, i.e. as $f_{\pm}/f_{ref}$, where f_{ref} is usually taken to be the value of $f_{\pm}$ at the lowest concentration measurement. The experimental and theoretical origins of this have been discussed respectively by Ise[42] and Muthukumar.[34] Thus, Muthukumar has shown that

substantial interactions between the polyions at very low concentrations both affect the polyion activity coefficient, f_p, where $f_\pm = [f_p f_x^\nu]^{\frac{1}{\nu'}}$, and the correlations that lead to the κ peak in the small angle scattering.[34]

The difficulty of the arbitrary value of f_0 disappears when $f_\pm$ is used in its differential form, i.e. as in the Gibbs equation, but it remains if two sets of data measured relative to different f_{ref} need to be combined. This is illustrated for protonated PSS in Figure 2(a), where mean activities measured by Dolar and Leskovsek[43,44] for HPSS at low concentrations are compared with measurements made by Ise and Okubo[45] at higher concentrations, each set referred to a different f_{ref}. To use them in the Gibbs equation the reference state of one or other of them has to be altered so that the whole set fits a single continuous function and that is what is attempted in the recalculated high concentration data in Figure 2(a). This seems to be the only system for which $f_\pm$ has been directly determined over a range that includes regions with and without counterion condensation. The activity coefficient data for NaPSS is more limited. However, the Manning expression, Eqn (5), can be used to calculate $f_\pm$ at low concentrations, using Figure S1, and the results combined with measurements at higher concentrations, just as done for HPSS, to give the approximate match of the two ranges of data for NaPSS shown in Figure 2(b). Also shown are the behaviour of $f_\pm$ and the result of applying the Gibbs equation in the form of Eqn (3) with a constant Γ_X of 1.0 μmol m^{-2}. Adsorption will not be constant in the real system but since the adsorption isotherm is mainly determined by the activity, it can be expected to be approximately constant in the concentration range up to about 10 mM and there is little change in the ST. However, by 10 mM the solution is fully in the semidilute region, where an increase in the bulk activity increases the magnitude of the ST gradient both directly, and indirectly, by increasing adsorption. This leads to a relatively sharp change in the slope of the Gibbs plot, sharper than observed in Figure 2(b), where only the first of these effects is shown. The change in slope in Figure 2(b) starts to occur at the value of c_r of approximately 1 mM calculated for a 500k PSS.[33,37] This suggests that the observations by Okubo[46] of a sharp

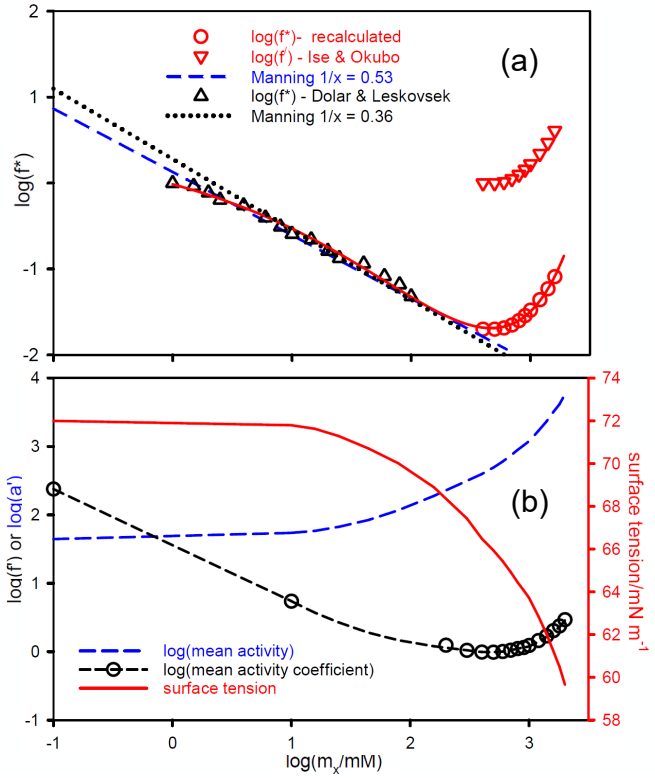

Figure 2: (a) Mean activity coefficient measurements, $f^* = f_{\pm}/f_{ref}$, for HPSS (MW = 200k at 273 K)[43] and HPSS (MW = 500k at 298K).[45] The latter are shown unscaled and rescaled to a common f_{ref} state by fitting to a single function. Manning models (Eqn (5) with fitted values of $1/\xi = 0.53$ and 0.36 are shown as dashed and dotted lines through the low concentration data. (b) Mean activity coefficient, mean activity and calculated ST for a 500k NaPSS at 298 K. The Manning model using $1/\xi = 0.36$ was used to fit concentrations below 10 mM and direct measurements[45] for the higher concentration data. The activity coefficient (points) was used to calculate the ST for a constant coverage Γ_X of 1.0 μmol m^{-2} using Eqn (3).

change in ST at a critical concentration c^* may have the same origin as that shown in Figure 2(b), i.e. $c^* = c_r$.

The surface equilibration of higher MW samples of PSS (70k) has been explored over the range 5 - 70 mM by Noskov et al. using dynamic ST measurements.[35] Equilibration of the ST was found to be extremely slow, requiring more than about 5 hr at all concentrations. After 5 hr the change in ST was found to be small at 5 mM but there was a much larger change

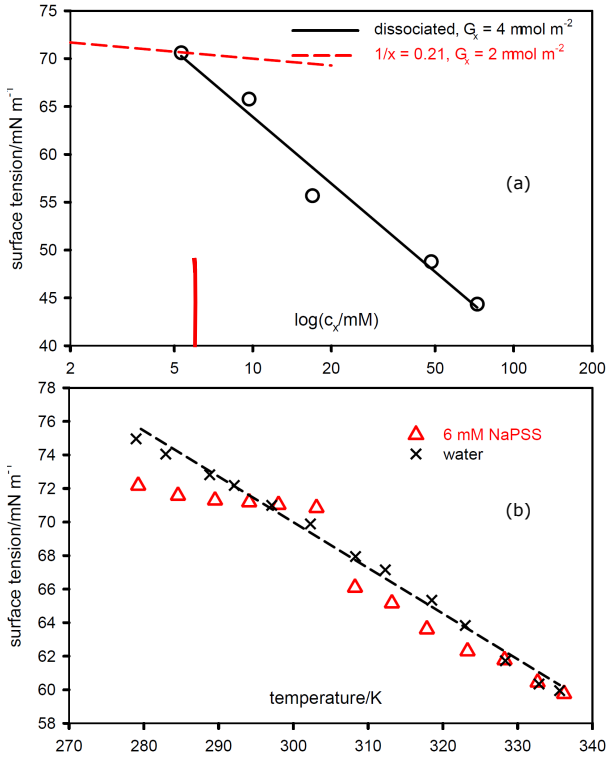

Figure 3: (a) Linear variation with $\log c_x$ of the extrapolated ST of solutions of 70k PSS equilibrated for 400 minutes, fitted using Eqn (3) for complete dissociation in the bulk solution and a constant Γ_X of 4 μmol m^{-2}. The dashed line is calculated for counterion condensation using Eqn (6) and a constant Γ_X of 2 μmol m^{-2}. The short vertical line (red) marks the concentration used for the plot in (b). (b) Variation of the ST of a 6 mM (monomer) solution of 70k PSS and water as a function of temperature. The measurement points and a linear fit are shown for water. The data are redrawn from Noskov et al[35] and (b) Natseh and Ayyad.[47]

at higher concentrations of about 20 mM. Although Noskov et al. did not give final ST values because equilibration was still not complete at any of their measured concentrations within the 400 min of the measurement, it is useful to examine the 400 minute values for comparison with the CG data above. To do this we have linearly extrapolated the last 2 or 3 measurements of Noskov et al. at each concentration to standardize the time of measurement to approximately 400 min. Figure 3(a) shows the resulting Gibbs plot. Figure S1 gives a value of $1/\xi$ of 0.21 for this MW, which combined with the gradient of the Gibbs plot would give a Γ_X of about 40 μmol m^{-2}, which is clearly unphysically large. However, if Eqn (6)

is assumed to hold only up to the c^r of about 5 mM, Eqn (3) must be used at the higher concentrations and this gives a more reasonable value of Γ_X of about 4 μmol m^{-2}. This is close to the value of 5 μmol m^{-2} obtained by direct measurement (neutron reflection) by Yim et al. for a 62k PSS in 0.67 M KCl.[48,48] Noskov et al. showed no measurements below 5 mM, but the results of Figure 1 and the sharp change in slope suggest that counterion condensation occurs below about 5 mM. Figure 3 includes as a dashed line the calculated plot for a lower Γ_X of 2 μmol m^{-2} but with counterion condensation and which agrees with the 1.7 μmol m^{-2} obtained from the data of Figure 1 for smaller MW PSS. Thus the sharp change of slope required to account for the relatively abrupt onset of surface activity can be accounted for in the framework of the activity measurements of Figure 2. Noskov et al. regarded the sharp change in ST as occurring at a concentration slightly higher than 5 mM and also identified it with the critical concentration c^* observed by Okubo and mentioned above. It agrees within error with the estimated c_r of 10 mM for this MW.[33]

Although the measurements above are consistent with counterion condensation, they do not resolve whether significant adsorption is still present in the concentration range less than about 10 mM , because this is concealed by the effects of counterion condensation on the ST gradient. A different approach to the ST measurement by Natseh and Ayyad more definitely points to adsorption of PSS coexisting with a negligible drop in ST from that of water.[47] As shown in Figure 3(b) and in agreement with Noskov et al. these authors observed little change in the ST at 6 mM from that of pure water. However, their experiment was an interesting variant in that they measured the ST of both water and the PSS (70k) solution as a function of temperature between 280 and 335 K. Their results were the same whether cooling or heating and whether measured with ring or plate. Although the differences in ST are small, the changes are systematic and could only be caused by adsorption of the polyelectrolyte.

All the above experiments on PSS were done without added electrolyte. Measurements for the addition of NaCl and KCl to NaPSS and KPSS for concentrations up to 70 mM and

for values of the X:MCl ratio of up to 5[49,50] have been shown to be approximately consistent with an expression derived by Manning.[25] However, the only ST measurements on PSS, in which the surface adsorption has also been directly measured, have been for high electrolyte concentrations. Yim et al.[48,51] used NR and ST to study two MW PSS (63k and 1300k) at the A-W interface, and there is some evidence from these measurements of the effects of counterion condensation on the surface. Thus, at a fixed concentration of 0.67M KCl and for the 1300k MW of PSS, Yim et al. directly observed substantial adsorption as a function of polymer concentration, as shown in Figure 4(a). Adsorption of 4-5 μmol m^{-2} was found at bulk concentrations of 5 mM and below, which *decreases* as the polymer concentration further *increases*. Yim et al. postulated that the drop in adsorption in Figure 4(a) was a result of the dilute-semidilute crossover value at c_r in 0.67 M KCl. However, their estimated value of c_r was 30 mM, which is towards the end of the drop in adsorption. Combining the values of c_r without added electrolyte from Nishida et al.[33] with recent comprehensive measurements of the dimensions of PSS in added NaCl[52] suggests that c_r for the 1300k of Yim et al. is 0.4 mM in the absence of electrolyte and about 4 mM in 0.7 M electrolyte. As shown in Figure 4(a) this puts the observed change in adsorption much closer to c_r. At 0.75M KCl the ST falls by about 4 mN m^{-1} as the polymer concentration increases from 5 to 50 mM (Figure 4(b)). The slope of the $\sigma - \log c$ plot in this concentration range indicates a nominal Γ_X of about 1 μmol m^{-2} for a Gibbs prefactor of one. The lack of an ST drop below 5 mM, even though the observed surface excess is substantial, is consistent with the behaviour in Figure 2, with the isotherm observed by Noskov et al,[35] and with the observations of Okubo discussed above, i.e. counterion condensation leads to a negligible slope in the ST below the c_r of about 4 mM for this MW, and above this concentration the slope approximately follows Eqn (3). Above about 4 mM the Gibbs factor is then 1 giving a Γ_X of 1 μmol m^{-2}. This agrees within error with the average value of 2 μmol m^{-2} measured directly by NR. From the point of view of establishing the exact effects of counterion condensation on the adsorption of PSS the results of Yim et al. do, however, show some other inconsistencies and there is

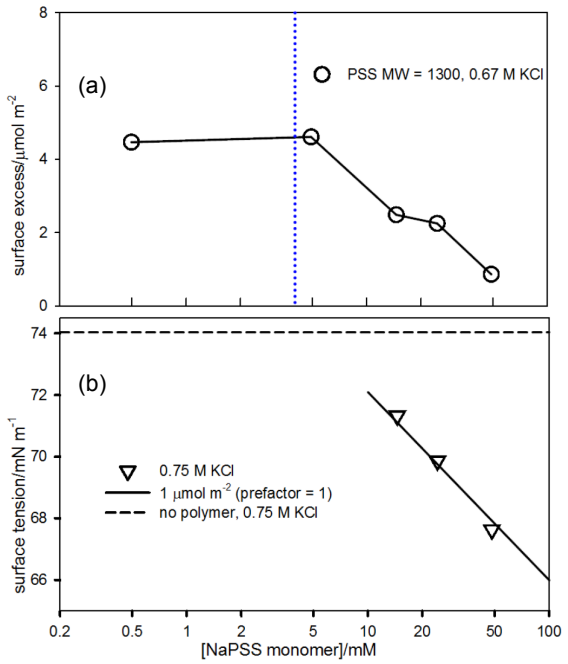

Figure 4: (a) Surface excess of PSS (1300k MW) in the presence of 0.67 M KCl as measured directly by NR, (b) ST as a function of concentration of the same polymer in the presence of no KCl and 0.75 M KCl. The blue dotted line marks the crossover of the dilute to the semidilute regime of the 1300k polymer in the absence of electrolyte. The data are redrawn from Yim et al.[48]

the possibility that equilibrium is not fully established for the large 1300k MW.

Yim et al. did not interpret their experiments as above but followed an earlier interpretation given by Frommer and Miller (FM). FM found a large apparent inconsistency between a high directly measured Γ_X and a high value of the ST for DNA.[53] Yim et al. and FM suggest that it is the desorption, i.e. negative adsorption, of simple electrolyte that counterbalances the depression of ST. Thus, if simple electrolyte is excluded from the adsorbed layer of polyelectrolyte the result is a negative Γ_X that will contribute to an increase in ST. Taking the thickness of the layer obtained by Yim et al. of 20 Å and an area per segment of 80 Å^2 (Γ = 2 μmol m^{-2}) gives a negative Γ_X in 1 M electrolyte of about 1 μmol m^{-2}. Given that the Gibbs prefactor would be 2 for the electrolyte this might significantly counteract the positive adsorption of PSS. Frommer and Miller found an adsorption of DNA of about 1 μmol m^{-2} at the lower concentration of 0.1 M NaCl. The dimensions of the polyelectrolyte layer were

not measured in their radiotracer measurement but, taking them to be comparable to those measured for PSS, would lead to a depletion of NaCl of only about 0.1 μmol m^{-2} which would be too small to cancel out the effect of the DNA adsorption on the ST.

Counterion Condensation and the Surfactant Binding Isotherm

The pattern of binding surfactants to polyelectrolytes can be approximately divided into two main regions. The first fraction of the binding occurs with relatively little increase in the free surfactant concentration, indicating a relatively constant binding energy per surfactant. However, for the next fraction the binding becomes steadily weaker and is therefore accompanied by a steady increase in the equilibrium free surfactant concentration. The ST directly depends on the activity of the surfactant through the Gibbs equation, and since the free surfactant concentration is often a good approximation for the activity in dilute solution, the ST is expected to change with concentration differently in the two regions. In the low concentration region the ST is approximately constant, irrespective of the adsorption, because of the behaviour of the free surfactant concentration, but in the higher concentration region the ST depends on both concentration and the surface excess. The range over which the ST is constant in the initial phase of the binding is defined by the start and finish of the initial binding regime. The form of the Satake-Yang equation,[54] which is commonly used to interpret binding isotherms, is such that it is particularly well suited to the parameterization of this initial binding regime. We write the equation as

$$\phi = \frac{\phi_{max}}{2}\left[1 + \frac{Ks_{free} - 1}{\sqrt{(1 - Ks_{free})^2 + \frac{4Ks_{free}}{\alpha}}}\right] \tag{7}$$

where ϕ is the fractional binding, K is a binding constant, s_{free} is the concentration of free surfactant, α is a cooperativity factor, and ϕ_{max}, which does not normally appear in the equation, is defined as the maximum cooperatively bound fraction. ϕ_{max} therefore empirically defines the region over which binding is cooperative. There are several possible

mechanisms for the cooperativity, which lead to different structural characteristics of the PE-S aggregates.[55,56] However, the nature of these structures has little direct significance for the surface behaviour, which is defined by the approximately constant free surfactant concentration and the range over which the revised S-Y equation holds, i.e. ϕ_{max}.

The revised Satake-Yang equation, which we denote by S-Y$_\phi$, then becomes an empirical equation that can in most cases be well fitted to the cooperative binding fraction with the two parameters K and α and the additional limiting factor ϕ_{max}. α is a measure of the *degree* of cooperativity and ϕ_{max} defines the *extent* of the cooperativity. We emphasize that ϕ_{max} is not the overall limiting bound fraction and we refer to surfactant bound at higher fractions than ϕ_{max} as non-cooperatively bound and not part of the description in terms of the S-Y$_\phi$ equation. The binding energy is commonly defined in terms of the critical aggregation concentration, CAC, or $1/K$ from the usual S-Y equation.[57] Our $1/K$ is not the same as in the original S-Y equation but it similarly corresponds to the value of s_{free} when cooperative binding of the surfactant on the polyion is half complete, i.e. at $\phi_{max}/2$. It therefore defines the mid concentration point of the ST plateau. If the cooperativity is high there is little difference between the values of $1/K$ defined by the two S-Y equations. In all the diagrams and discussion that follow, we use this different definition of $1/K$, which lies somewhere between the CAC and the normal S-Y value of $1/K$.

The variation of values of $1/K$ for some PE-S complexes are plotted against surfactant chainlength in Figure 5. Although electrolyte concentration changes $1/K$, the effects of NaCl for the comparison here are relatively small. The systems in Figure 5 typically have values of $1/K$ about two orders of magnitude lower than the normal CMC when polyelectrolyte is added. The relative change noticeably increases with chainlength. Konop and Colby[61] have shown that the entropy gain of the counterions liberated from a polyelectrolyte segment when it binds to the surfactant micelle is a key factor in driving complexation. It approximately cancels all the other entropy losses so that the nett effect on the free energy of micellization is just the hydrophobic gain on aggregation (but see Hansson[63] for a fuller discussion). Hence

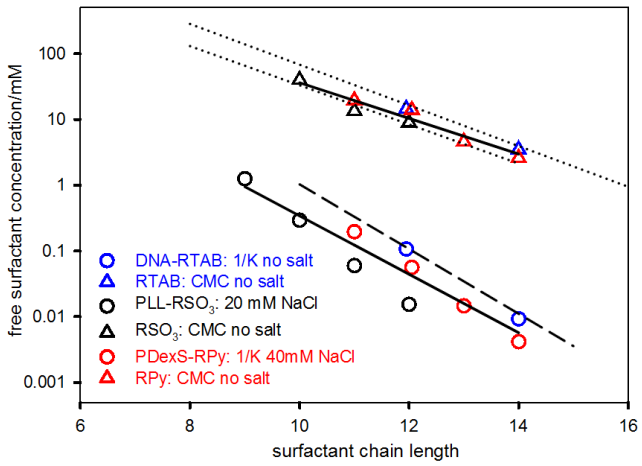

Figure 5: CMCs and reciprocal binding constants ($1/K$) for surfactants of different chain length. The systems are PDexS with alkyl pyridinium chlorides (RPy),[58] DNA with alkyl TABs (RTAB),[59] and poly(L-lysine) (PLL) with alkane sulfonates (RSO_3).[60] The dotted lines are the CMCs of alkyl TABs and alkyl sulfates, and the dashed line is the CMCs of octaethylene glycol monoalkyl ethers (C_nE_8), following Konop and Colby.[61] Values of the CMCs for alkyl TABs and alkane sulfonates are from van Os et al.[62]

the magnitudes of the chain dependences between PE-S complexes and nonionic surfactants are similar, as shown in Figure 5. Konop and Colby further show that the addition of simple electrolyte reduces the gain in entropy on release of counterions from the polyelectrolyte fragment attached to the surfactant aggregate and therefore causes aggregation to occur at a higher concentration. This shift is shown for three different systems in Figure 6. However, although the addition of electrolyte increases $1/K$, the curves become steeper and ϕ_{max} increases, suggesting more cooperative and more extensive binding at higher electrolyte concentrations. This increase may result because an aggregate is both bound to a polyion segment and has some residual exposure to free ions. Thus, addition of electrolyte enhances aggregate formation but it destabilizes polyion attachment. The former mainly determines the degree of cooperativity but the latter dominates its extent. Hansson and Almgren[64] have, however, attributed this solely to an increase in the binding constant. The enhancement of ϕ_{max} by added electrolyte occurs for many, but not all PE-S systems.

Divergences from the S-Y equation above ϕ_{max} have mostly used binding models that

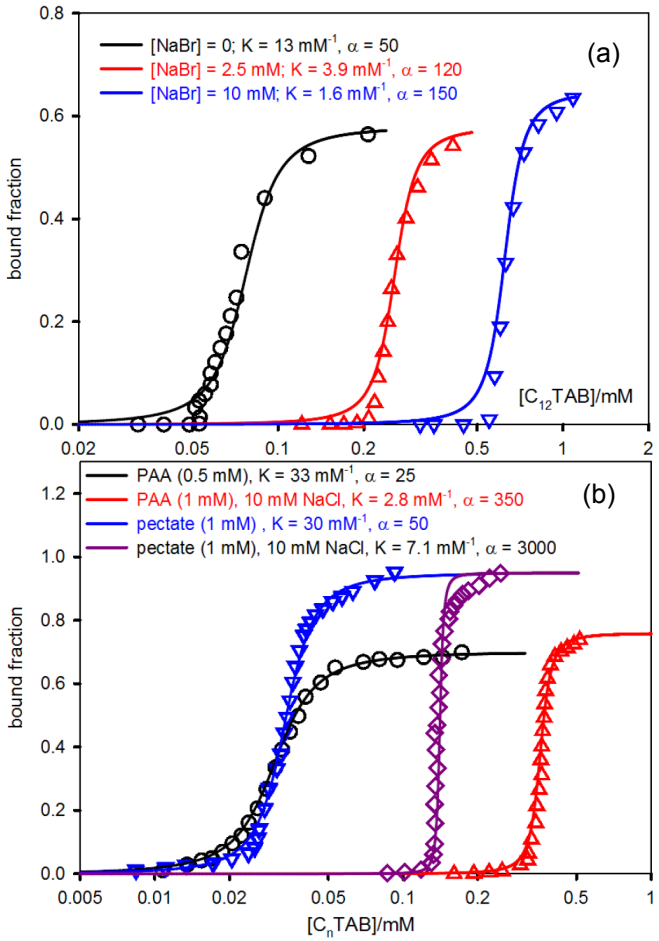

Figure 6: Observed and calculated binding curves for the binding of (a) C_{12}TAB with sodium poly(carboxymethylcellulose) (CMC) (MW = 95k, $\xi = 3$, $c = 0.5$ mM) in different concentrations of added electrolyte (NaBr), and (b) C_{12}TAB with PAA with and without added NaCl and C_{14}TAB with pectate with and without added NaCl. The fitted curves use Eqn (7) with the values of K and α given in brackets and an adjustable ϕ_{max}. Data are redrawn from Hansson and Almgren[64] and Hayakawa et al.[65]

extend beyond the simple nearest neighbour interaction used in the S-Y equation, e.g.[66–69] However, Hayakama and Kwak suggested that binding consists of the cooperative replacement of counterions by surfactant ions, with the implied result that $\phi_{max} = (1 - 1/\xi)$. Although there is no simple relation between ϕ_{max} and $1/\xi$, the binding curves shown in Figure 7 (low $1/\xi$ in (a) and high $1/\xi$ in (b)) suggest that surfactant binds preferentially to polyelectrolyte segments *not* involved in counterion condensation, which is the reverse of Hayakawa and Kwak's mechanism. This would make surfactant and counterion condensa-

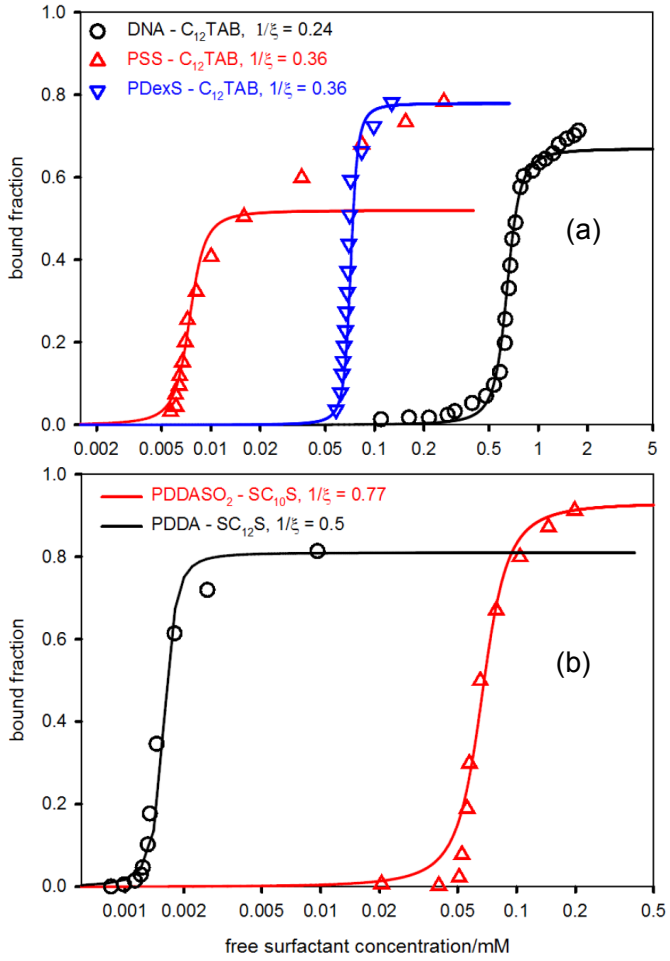

Figure 7: Observed and calculated binding curves for (a) DNA + C_{12}TAB in 20 mM NaCl[59] ($\beta_{max} = 0.67$, $K = 1.55$, $\alpha = 110$), PSS + C_{12}TAB in 21 mM NaCl[70] ($\phi_{max} = 0.52$, $K = 200$ mM^{-1}, $\alpha = 130$), poly(dextran sulfonate) PDexS + C_{12}TAB in 20 mM NaCl[70] ($\phi_{max} = 0.78$, $K = 14$ mM^{-1}, $\alpha = 400$), and (b) PDDA-SDS in 1 mM NaCl[71] ($\phi_{max} = 0.81$, $K = 630$ mM^{-1}, $\alpha = 200$), and PDDASO$_2$ - $SC_{10}S$ in 20 mM NaCl[72] ($\phi_{max} = 0.93$, $K = 15.0$, $\alpha = 40.0$). The values of ξ are from Li and Wagner[19] except for PDDASO$_2$, which is estimated from the additional length of inserting an SO_2 group in the PDDA structure.[30,31]

tion competitive, in which case $\phi_{max} \approx 1/\xi$ (or 1 when there is no counterion condensation). When $1/\xi < 1$ and surfactant binding is sufficiently strong, surfactant might also be expected to displace counterion from condensate domains to some extent. Thus, a strong interaction of surfactant chains with the hydrophobic backbone or with each other might then erode or destroy domains of counterion condensate.

In counterion condensation the counterions lose their bulk translational entropy, which

opposes the condensation, but this is partly offset by the retention of some ion mobility in the condensate, and the condensate therefore remains stable as the concentration falls to zero and does not dissociate as required by the law of mass action. The tendency of surfactant ions to cluster and/or to become more localized by binding to the hydrophobic backbone of the polymer might swamp the delicate entropy-electrostatic balance that creates the counterion condensate. The extra stability of PE-S complexes resulting from the gain in entropy of counterions displaced from an attached polyelectrolyte segment is only applicable to counterions that are not part of the condensate. It is unlikely to apply to condensate ions because loss of a counterion from the condensate would lead to an insignificant gain in entropy and would adversely affect the overall electrostatic energy of the polyion-condensate. Nevertheless, there are indications that surfactant ions do sometimes behave like normal counterions and may even participate in counterion condensation,[73] which we discuss below.

The differences in ϕ_{max} in Figure 7 are sensitive not just to the fractional charge but also to unknown factors associated with the hydrophobic natures of polyelectrolyte and surfactant. That ϕ_{max} can be lower than 1 is shown particularly clearly by the binding isotherm exhibited by PSS-C_{12}TAB in Figure 7(a) where the S-Y equation only fits the data up to a $\phi_{max} < 0.5$. The remaining binding is clearly different and the existence of two quite different binding regimes is the key to understanding the surface behaviour of PE-S complexes as we now discuss.

Polyelectrolyte-Surfactant Mixtures at the Air-Water Interface

The Surface Tension of PE-S Complexes: the Low Concentration Region

The mixing of polyelectrolytes and oppositely charged surfactants lowers the ST at concentrations too low for either species to be strongly surface active, but this does not happen in a regular manner. At high surfactant concentrations, i.e. approaching and above the normal CMC, the free surfactant dominates the ST behaviour, which then resembles that of free surfactant. Between these two regions the ST may vary strongly and erratically. Some of

this intermediate region typically involves precipitation of a PE-S complex of approximate stoichiometry 1:1 S:X where X is the polymer monomer, followed by resolubilization as more surfactant is added. Both precipitation and resolubilization are affected by problems of equilibration. We start by examining the concentration region below precipitation.

The Gibbs equation in the form of Eqns (1) - (3) applies when a polyelectrolyte adsorbs as the neutral species PY_ν and the activity is that of bulk PY_ν regardless of the state of either dissociation or counterion condensation, i.e. the polyelectrolyte behaves as a single component. However, this feature is lost in a PE-S system because the adsorbed complexes have a range of composition and surface activity, and surface neutrality can be achieved by adjusting the balance of S and Y ions between bulk and surface species. The application of the Gibbs equation therefore requires a knowledge of the variation of the surface activity of each stoichiometric species as well as of the activity of their bulk complexes.

In the region below precipitation, i.e. at stoichiometries lower than about SX, the surface activity of a bulk complex $S_\phi X$ should be low when ϕ is much less than 1 because the extended polymer chain at the surface would lead to a large spacing between surfactant molecules, which does little to shield the high energy water surface from air. When ϕ is much greater than 1 the excess bound surfactants may lead, for example, to an extended structure that is effectively a hydrophobically coated rod, or to a collapsed structure with clusters of surfactant within a coiled polymer configuration, neither of which is likely to be active at the A-W interface, although there are other configurations that could be strongly surface active. Where the surface composition has been experimentally determined by NR, each system is found to have its own preferred surface stoichiometry, γ, with a value that lies approximately in the range $1/2 < \gamma < 2$ and which varies negligibly with *overall* stoichiometry over most of the concentration range of interest. The invariability of γ indicates that bulk complexes with values of ϕ different from γ are significantly less surface active . In such a situation and if $\gamma \approx 1$, the same form of the Gibbs equation as used for polyelectrolytes, i.e. Eqns (1)

- (3), will be an appropriate approximation. Eqn (3) then becomes

$$d\sigma = -\Gamma_S RT d\ln c_\pm f_\pm \approx -\Gamma_S RT d\ln s_{free} \tag{8}$$

where the concentration of surfactant is approximated to the concentration of free surfactant as distinct from total surfactant, s_{total}. Although Γ_P does not appear explicitly in this equation, the polymer contribution is in the value of $f_\pm$, and although the right hand side of Eqn (8) neglects ionic contributions to $f_\pm$, it does include the dominant contribution, which arises from aggregation, and which is determined experimentally in measurements of the binding curve. Eqn (8) is probably also an adequate approximation for the ST when γ is not too much larger than 1. For a value of γ less than 1, however, the bulk concentration of the surface active species may start to decrease before precipitation is reached. In this case Eqn (8) may only be a valid approximation up to $\phi = \gamma$. The change in behaviour when the overall stoichiometry reaches γ may then be particularly marked if γ is in the vicinity of the cooperative-noncooperative binding changeover in the bulk at ϕ_{max}. This may lead to sharp changes in the bulk activity of the dominant surface species and hence in the ST. We discuss this in detail after applying Eqn (8) to various experimental data.

Eqn (8) simplifies in an interesting way when the binding isotherm is divided into its cooperative and noncooperative ranges. Figure 8 shows a plot of $\log s_{free}$ against $\log s_{total}$ using data from one of the measured binding curves for NaPSS-C_{12}TAB[70] in Figure 7(a). The slope of this plot is required to convert Eqn (8) into a correct Gibbs plot in terms of s_{total}, and it shows that $\log s_{free}$ is close to being constant during cooperative binding but becomes a much steeper linear function of $\log s_{total}$ in the non-cooperative binding region. Consequently, when substituted into Eqn (8) and combined with a constant value of the coverage the ST is approximately constant with s_{total} during cooperative binding and then decreases strongly during non-cooperative binding. The ST as a function of s_{total} consistently follows such a pattern for PE-S systems and the basic features of Figure 8 are usually clear in the raw

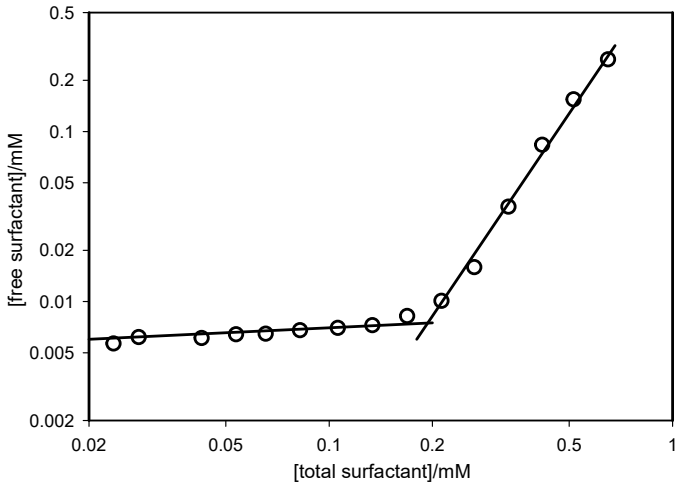

Figure 8: The relation between free and total surfactant concentrations in a binding isotherm for NaPSS-C_{12}TAB in 20 mM NaBr. The data are from Hayakawa and Kwak.[70]

data of a surfactant electrode determination of the binding curve (see, for example, Figure 5 in Hansson and Almgren[73]). The low concentration region therefore divides naturally into three regions, A, where no bulk complex at all is formed in solution, B, which spans the range of cooperative binding in the bulk, and C, which spans the range of non-cooperative binding and which may finish at or close to precipitation.

The ST profiles, the surface excesses as determined directly by NR, and the binding curves of PSS-C_{12}TAB with and without added simple electrolyte are shown in Figure 9. The MW for these measurements was 18k, the concentration was 0.7 mM (140 ppm), well below the c_r of 130 mM, and the added electrolyte was 100 mM NaBr. Data are also shown for a polymer concentration of 0.1 mM (20 ppm). Hayakawa and Kwak measured $1/K$ as a function of added NaCl[70] and we have interpolated their data to obtain the binding isotherms at 0 and 100 mM NaCl, making the assumption that NaCl and NaBr have similar effects. We have combined this with the measured dependence of $1/K$ on polymer concentration[18,57,73] to obtain the final binding curves for 0.7 mM monomer without electrolyte shown in Figure 9(c). Binding curves are normally plotted as a function of s_{free} and Figure 9(c) shows both this plot and the plot as a function of s_{total}. The two concentrations of polymer illustrate

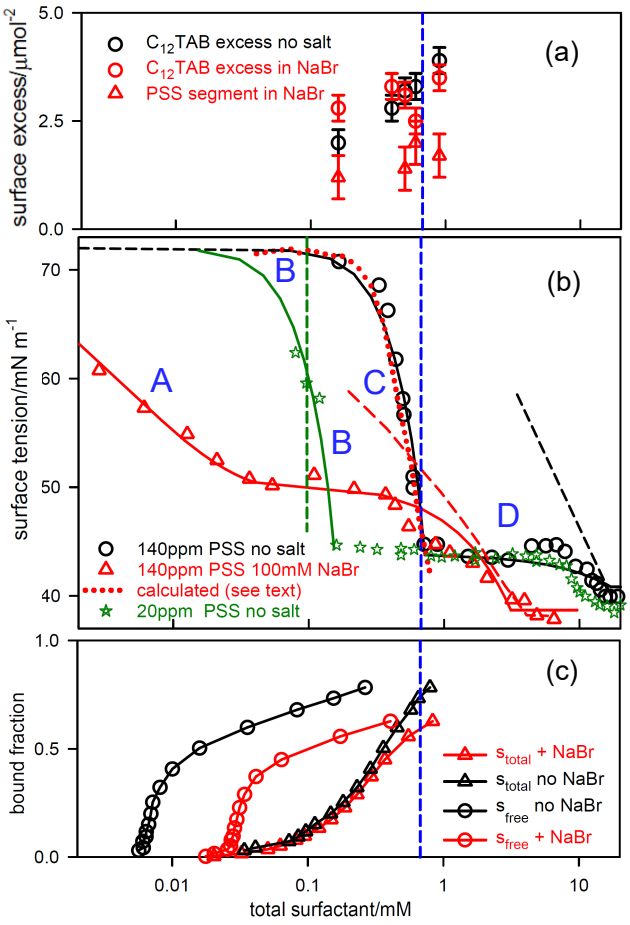

[t]

Figure 9: (a) Surfactant and polymer surface excess, (b) surface tension,[74–76] and (c) binding curves for PSS-C_{12}TAB with and without 100 mM NaBr.[70,73] Two concentrations of PSS (MW = 18k) are shown, 140 ppm (0.7 mM) with and without electrolyte, and 20 ppm (0.1 mM) without electrolyte. The fits in (b) are calculated by Bahramian et al.[15] and are here to guide the eye. The equivalence points for 20 and 140 ppm (total [X] = total [S]) are the vertical dashed lines. The binding curves in (c) are plotted against either s_{free} or s_{total}. A, B, C and D designate regions of surface behaviour for the 140 ppm sample and the red dotted lines in (a) and (b) are fits described in the text.

the concentration dependence of the ST that was identified as characteristic of Type 1 surface behaviour. The slightly different relative position of the steep drop in ST and each equivalence point is discussed in more detail below.

The lowest concentration ST measurements for PSS-C_{12}TAB without electrolyte start at an s_{total} above the onset of binding, i.e. in region B, for which Figure 8 and Eqn (8) show that the ST should vary relatively little with s_{total}. Thus, even if there is no adsorption of

PE-S complex directly from the fully dissociated state in solution, it is possible for there to be significant adsorption but little depression of the ST at the onset of B. , as mentioned above. The measured surface excess (NR) at the high concentration end of B in Figure 9(b) does indeed show significant adsorption. Parallel results for other systems confirm such adsorption over a wider range and are shown below. The polymer itself is expected to be initially in the counterion condensed state and since this only affects the ST through its effect on the mean activity of the complex, there may also be significant polymer only adsorption in the initial solution with little change in the ST (Figure 2(b)).

At the end of region B in the absence of electrolyte the ST develops an unusually steep negative gradient[15] in region C. This coincides with the end of the cooperative part of the binding isotherm and, as shown by Figure 8, Eqn (8) requires the ST to drop sharply. The gradient of this drop is also affected by changes in surface coverage and by the presence of any counterions. A linear fit of the measured surface coverage, shown as a red dotted line in Figure 9(a), was used here with the experimental variation of s_{free} with s_{total} to calculate the ST isotherm, also shown as a red dotted line in Figure 9(b). Direct measurement of the composition by NR gives a stoichiometry of the adsorbed complex of approximately S_2X. There is then the possibility that S_2X must become S_2XBr at the surface, which would further increase the gradient. However, inclusion of the effect of a Br^- counterion is within the experimental error of the slope of the experimental surface excess. Despite this uncertainty, the steepness and the onset of the ST are well explained by Eqn (8), which supports its use in a case when γ in $S_\gamma X$ is greater than one. That the onset of phase separation (precipitation) occurs at the end of the steep slope in ST has been established by several authors, particularly Hansson and Almgren.[20,73] The ST forms an approximate plateau in region D, as required by the Gibbs equation for precipitation of a surface active precipitate (the spreading pressure of the PSS-C_{12}TAB precipitate is known to be high[77,78]). We discuss the transition between C and D regions in more detail below.

In electrolyte the onset of binding shifts to a substantially higher concentration so that

there is no bound complex in solution at the lowest concentration measurements. However, the added electrolyte also stabilizes charges at the interface and therefore enhances adsorption of ionic species. This combination now causes the ST to start to decrease in region A, where it obeys Eqn (8) with $s_{free} = s_{total}$ and the system therefore behaves like a surfactant on its own in excess electrolyte, except that in the PE-S case adsorption of surfactant requires co-adsorption of PSS. The pattern for region A is similar to that previously applied by Buckingham et al. to the ST of poly(L-lysine)-SDS mixtures.[79] Applying Eqn (8) to the initial slope in Figure 9(b) gives a surface excess of surfactant of 2 μmol m^{-2}, which is reasonable considering the level of adsorption of segments of the pure polymer (1.7 μmol m^{-2}) and the direct NR measurement of surfactant (an average of about 2.5 μmol m^{-2}) and polymer (average of about 1.5 μmol m^{-2}) in region B. In electrolyte the change from a decreasing ST in region A to the near plateau in region B coincides with the onset of cooperative binding (Figure 9(c)) and, as already shown in Figure 8, Eqn (8) for this region must have a low ST gradient. This results in the unusual situation that the change from region A to B is concave with respect to the axes, which normally does not occur in a Gibbs plot.

Figure 10 shows the binding and ST data for PDDA-SDS without electrolyte. NR again shows that adsorption of SDS occurs in region B at concentrations where the SDS would not adsorb on its own. This adsorption also does not lower the ST significantly because of the nearly constant activity of the surfactant in the bulk solution (Figure 10(c)). Just as for PSS-C_{12}TAB, the sharp change in slope between regions B and C can be attributed to the switch away from cooperative binding. The B-C transition occurs at a higher relative concentration than for PSS-C_{12}TAB because cooperative binding extends to a higher ϕ_{max} of about 0.7 (see Figure 7) and this also causes the B-C changeover to be closer to the equivalence point (total [X] = s_{total}). Although the data here are less complete, the B-C region of the ST curve can again be quantitatively fitted to Eqn (8) using the surface excess, surfactant activity and ST data. Thus, the last pair of points in the experimental binding curve, which are above ϕ_{max}, extrapolate to give the variation of s_{free} shown as the red

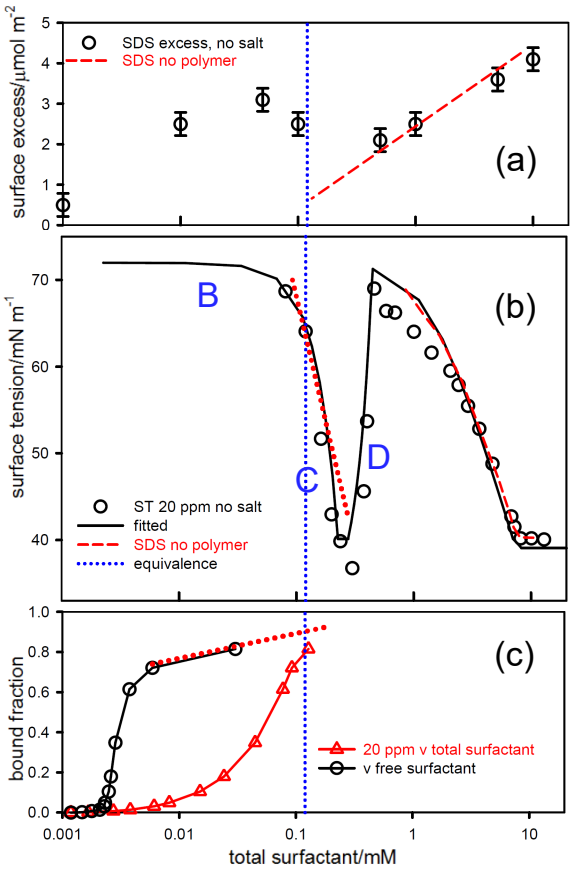

Figure 10: (a) Surfactant surface excess,[80] (b) surface tension at 20 ppm (0.12 mM) PDDA (MW = 100k),[80] and (c) binding curves for PDDA-SDS at 303 K, all in the absence of electrolyte.[71,81,82] The fits in (b) are those calculated by Bahramian et al.[15] and are here to guide the eye. The ST curve for the surfactant in (b) is shown as a dashed line and the equivalence point as a dotted line. The binding curve is plotted separately against s_{free} and s_{total}. The red dotted lines are explained in the text.

dotted line in Figure 10(c). This combines with the mean surface excess to give the ST variation shown as the red dotted line in Figure 10(b). The sharp increase in ST in region D probably results from a loss of the dominant surface active complex SX_2 when the overall stoichiometry increases above SX_2, and is discussed further below.

The equivalent data are shown for PDDA-SDS with added electrolyte for two polymer concentrations in Figure 11. The effect of adding electrolyte is again that the CMC of the free surfactant is lowered from about 8 to 1 mM, the CAC is raised by an even larger factor, and adsorption of the dissociated complex is favoured. The combined region B + C is short for

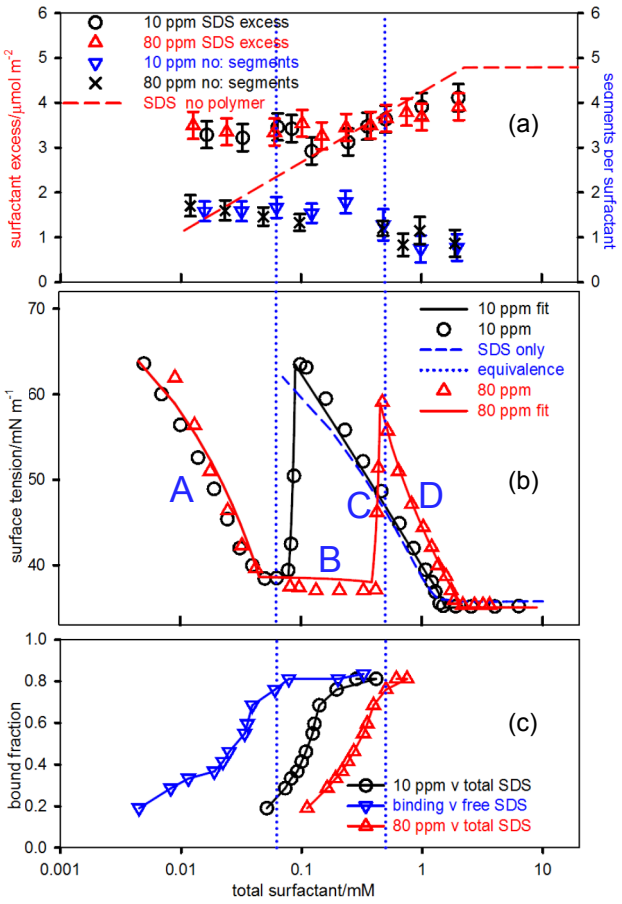

Figure 11: (a) Surfactant excesses and number of polymer segments per surfactant,[83,84] (b) surface tension,[83] and (c) binding curves[85] for PDDA-SDS at two polymer concentrations of 10 and 80 ppm in 100 mM NaCl. The fits in (b) are those calculated by Bahramian et al.[15] and are here to guide the eye. The ST curves for the surfactants on their own are shown as dashed lines and the equivalence points as dotted lines. The binding curves in (c) are shown plotted against s_{free} and against s_{total}. The regions A, B, C and D refer to the 80 ppm sample.

10 ppm polymer but more extended for 80 ppm simply because the latter requires 8× more surfactant. The effects of the increase in CAC and decrease in CMC mean that regions C and D are squeezed into a narrow range of concentration and it is not possible to define their division. Unfortunately, the combination of this narrow concentration range with a less well defined binding curve allows only an approximate analysis (there is no binding data below $\phi = 0.2$). The binding curve of Nizri et al. in 100 mM NaCl is, however, semi-quantitatively consistent with the overall pattern of ST behaviour. The large difference between Figures

11(b) and 10(b) results mainly from the increase in the CAC on adding 100 mM NaCl. In electrolyte the initial ST is therefore in region A where there is adsorption but no bound complex in the bulk solution, and region B becomes a low ST plateau but with a similar level of adsorption. The changeover between A and B occurs at the onset of binding, as expected. In the absence of electrolyte the onset of binding is known from the binding curve measurements to be independent of polymer concentration.[71,81,82] However, the polymer concentration independence of the A-B transition itself also shows that $1/K$ also does not depend on polymer concentration in the presence of 100 mM NaCl.[20] Again, the sharp peak at the onset of region D probably arises from the low surfactant stoichiometry of the surface active complex. This and the the switch between cooperative and non-cooperative binding, which is experimentally less well defined than in the absence of electrolyte, are discussed further below.

The effect of polymer concentration and added electrolyte show clearly that when the initial drop in ST is caused by the onset of binding in the bulk, it is independent of polymer concentration, i.e. $s_{total} \approx s_{free}$, but when it is caused by the switch from cooperative to non-cooperative binding it is approximately proportional to the polymer concentration ($s_{total} \propto$ [X]s_{free} (see Figure 8). By enhancing the adsorption of dissociated complexes, the addition of electrolyte contributes significantly to the initial polymer independent drop in ST. Changing the surfactant chain length changes the CMC and CAC in the *same* direction, which has a totally different effect from that of adding electrolyte, where the CMC decreases while the CAC increases. The directly measured surfactant excesses and the ST of $SC_{10}S$ with 20 mM PDDA are shown in Figure 12 with and without 100 mM NaCl. The value of $1/K$ has not been determined experimentally but its value can be estimated using the variation in Figure 5 and the measured value for PDDA-SDS. In added electrolyte, the ST starts in region A below the onset of bulk binding and then progresses as expected to a region B plateau corresponding to cooperative binding. The further progress to a sharp increase in ST, as for PDDA-SDS with electrolyte, is masked by the CMC of the surfactant being

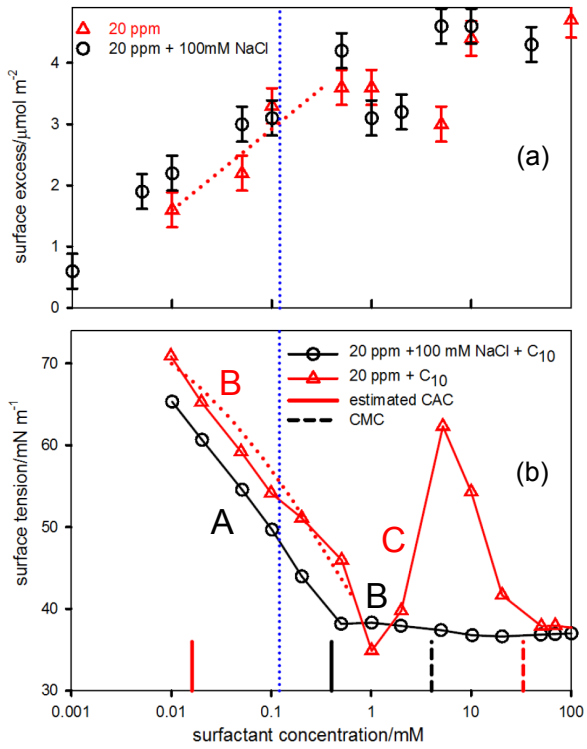

Figure 12: Surfactant surface excess measured directly with NR (a) and ST (b) for $NaC_{10}S$ with 20 ppm PDDA with and without added 100 mM NaCl.[80] The equivalence point is shown as a vertical blue dotted line and the short vertical lines mark the CMC (dashed) and estimated CAC ($1/K$).

reached before region C so that the free surfactant dominates the ST. However, the ST peak in region C/D does appear when there is no added electrolyte because the CMC is then much higher. An interesting feature of the system without electrolyte is that the initial slope in region B is similar to that with electrolyte and can also be fitted using the directly measured surface excess and a Gibbs prefactor of 1 (red dotted lines in the figure). Strong cooperative binding would give a plateau in the B region but the binding of the less hydrophobic $SC_{10}S$ is evidently sufficiently less cooperative than for SDS that the ST becomes characteristic of a system with non-cooperative binding.

The parallel results for PDDA-$SC_{14}S$ are shown in Figure 13. Given the strong decrease in cooperative binding on changing from C_{12} to C_{10}, there should be a corresponding increase in cooperativity in changing from C_{12} to C_{14}, and this is what is observed. Thus, direct mea-

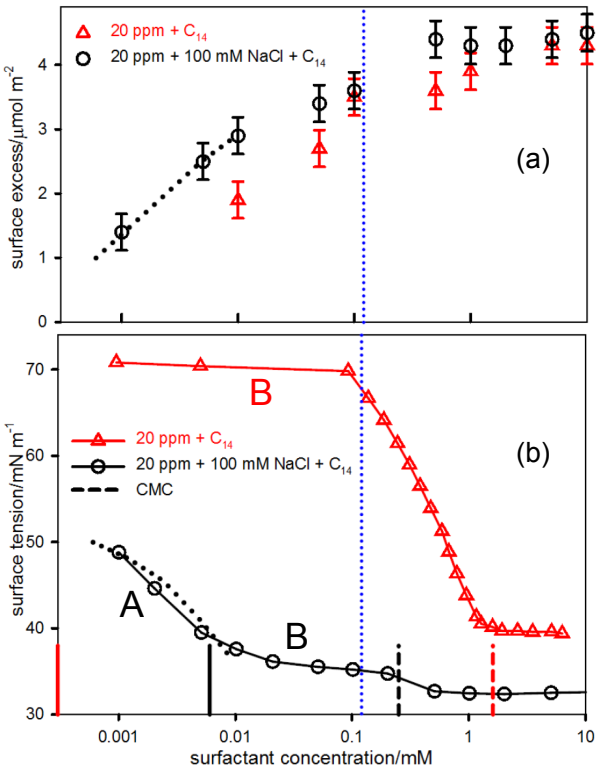

Figure 13: Surfactant surface excess measured directly with NR (a) and ST (b) for $NaC_{14}S$ with 20 ppm PDDA with and without added 100 mM NaCl.[80] The equivalence point is shown as a vertical blue dotted line and the short vertical lines mark the CMC (dashed) and estimated CAC ($1/K$).

surement of the surface excess shows strong adsorption of surfactant at low concentrations when there is no electrolyte but the ST remains high, as is appropriate for cooperative binding (region B). The increase in chainlength also leads to a low CMC, which is almost at the equivalence point. The system is therefore still in the B region when the free surfactant starts to dominate the ST behaviour. When electrolyte is added the initial ST measurements are below the onset of binding and pattern A occurs over a short range before cooperative binding leads to a B region plateau, again because of strong cooperativity. The level of adsorption is consistently higher when 100 mM NaCl is added. This is the normal effect of added electrolyte on surfactants at the A-W interface, in contrast to its effect on $1/K$.

The division of the general pattern of adsorption into the four regions A, B, C and D is further emphasized by considering the effects of cooperativity on the Gibbs equation. The

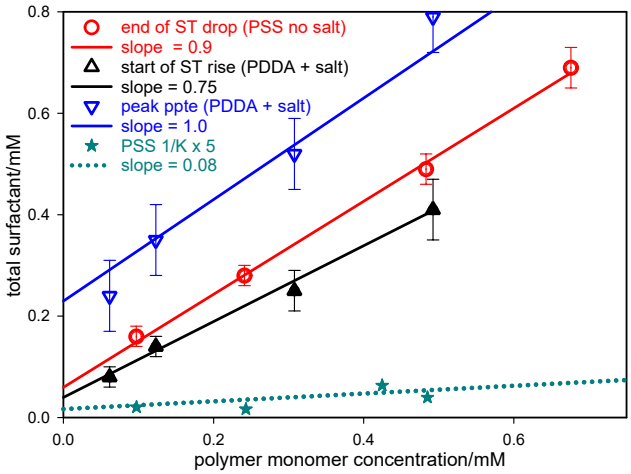

Figure 14: Plots of the total surfactant concentration at the onset of various changes against polymer monomer concentration for PSS-C_{12}TAB (precipitation),[74] PDDA-SDS with 100 mM NaCl (onset of ST upturn),[83] PDDA-SDS with 100 mM NaCl (maximum precipitation),[83] and of the initial aggregation defined by $1/K$ for PSS-C_{12}TAB.[18,57,73] For the latter the fitted slope includes a point not shown at 4.8 mM polymer monomer.

two simplest cooperative processes for surfactant on its own are precipitation and micellization. If the ST is plotted against $\log a_s$ for a sparingly soluble surfactant below its Krafft temperature, it decreases as the solubility limit is approached and the plot ends abruptly at precipitation. If plotted against $\log s_{total}$, as is done for PE-S systems, the abrupt ending becomes a horizontal straight line because the ST is not affected by adding excess precipitate. The surface excess, Γ, of surfactant also remains constant as $\log s_{total}$ increases, although this is masked by the zero change in $\log a_s$ with s_{total} above precipitation. Thus, there is a discontinuity in the ST gradient but not in either Γ or the ST. Micellization is not a true phase change but the more limited cooperativity still leads to a discontinuity in the ST gradient. However, the gradient does not become zero above the CMC and Γ is not constrained to be constant. Below the CMC $a_s \approx s_{total}$ but above the CMC s_{total} includes the aggregated surfactant and therefore the activity of the monomer ($\approx s_{free}$) is much less than s_{total}, which substantially reduces the magnitude of the ST gradient above the CMC. In the cooperative binding of surfactant to a polyelectrolyte, aggregation takes place in two notional steps, which are the initial binding and the subsequent formation of aggregates.

If we assume that, as for micellization and precipitation of the free surfactant, aggregation occurs at a well defined value of the surfactant activity (taken to be $\approx s_f^*$) and corresponding bound fraction (ϕ^*), then the value of s_{total}^* at aggregation is given by

$$s_{total}^* = s_f^* + \phi^*[\mathrm{X}] \tag{9}$$

where [X] is the total concentration of polymer monomer in the system. Eqn (9) can be used to assess cooperative processes in PE-S systems. Thus, Figure 14 shows Eqn (9) applied to (i) the base of the sharp drop in ST in PSS-C_{12}TAB, (ii) the base of the onset of the ST rise in PDDA-SDS with electrolyte, (iii) the point of maximum precipitation in PDDA-SDS with electrolyte, as identified by Staples et al.,[83] and (iv) the initial aggregation in PSS-C_{12}TAB as defined by $1/K$.[73] Precipitation for a fully charged polyelectrolyte should have a slope of 1. However, most PSS samples are quoted as being 90 or 95% sulfonated and the observed slope of 0.9 for the base of the sharp drop in ST for PSS-C_{12}TAB is therefore within error of the value expected for the onset of precipitation. The maximum precipitation of PDDA is less accurately determined because it occurs over a broad region, but it is within error of the expected value of 1. The value of 0.75 for the upturn in ST for PDDS-SDS is less consistent with precipitation and we discuss it further below. For PSS-C_{12}TAB the intercept of the plot of $1/K$ shows that a small fraction of polymer of about 10% is taken up before the onset of cooperative binding. This fraction may be bound as individual molecules or as surfactant ions incorporated into the counterion condensate (for a further discussion see Hansson and Almgren[73]). It would also mean that the ST would not initially be lowered significantly on the addition of this amount of surfactant, even if some surfactant is adsorbed at the surface. PSS-C_{12}TAB appears to be unusual in this variation of $1/K$ with polymer concentration.

Surface Tension Behaviour in the Intermediate Concentration Region D

At the start of region D the ST is dominated by the PE-S complex but by the end it is dominated by surfactant. In systems such as PSS-C_{12}TAB (Figure 9) the start is the onset of the ST plateau that signals phase separation (precipitation), but in PDDA-SDS with electrolyte it starts with an ST peak. Such a peak is characterized by a relatively sharp and significant increase in the ST at the onset of the peak. The drop in ST on the high concentration side of the peak is usually dominated by the surface activity of the significant fraction of free surfactant that builds up during and after the resolubilization of the polymer precipitate. As already discussed, the Gibbs equation does not allow precipitation on its own to cause a step change in the ST, although for a PE-S system a change in the gradient is allowed. The positive ST gradient required for the onset of an equilibrium ST peak must therefore result from either a decrease in the bulk concentration/activity of the preferred surface active species as s_{total} increases or from a negative surface excess of solute at the surface, such as occurs in simple ionic solutions. NR shows unequivocally that there is a positive excess of complex during these changes. Thus, either the activity of the main surface active species decreases at the onset of the peak or the effect is a non-equilibrium one.

Where the surface stoichiometry has been determined experimentally, the surface adsorbed species, $S_\gamma X$, has a particular stoichiometry for each system, which is independent of the overall stoichiometry over the concentration range of interest. For example, γ is approximately 1/2 for PDDA-SDS and 2 for PSS-C_{12}TAB. Since the compositions of the bulk complexes vary over a wide range during addition of surfactant, the constancy of the surface composition establishes that the spread of stoichiometry of the surface active complexes must be narrow, because surface activity has a highly selective effect on surface composition, e.g.[86,87] It is also not surprising that complexes with stoichiometries between 0.5 and 2 surfactants per monomer are not surface active. At low stoichiometry the surfactants will be too far apart to screen high ST water from air, and at high stoichiometry they will tend to form either an extended hydrophobic rod, or a three dimensional structure of surfactant

aggregates, neither of which is likely to be surface active. A further feature is that in the only case where the effect of added electrolyte has been tested the surface stoichiometry was found to be insensitive to electrolyte.[74–76] Again this is not surprising, because the surface activity should largely be determined by the stereochemistry of the head group-segment interaction.

The composition of the bulk complexes varies over a wide range. Up to $\phi = 1$ it depends on the balance between cooperative and non-cooperative binding and the value of the changeover at ϕ_{max}. At higher concentrations and when precipitation is of the 1:1 complex, the average stoichiometry of the bulk complexes will increase beyond $\phi = 1$ as extra surfactant binds during the resolubilization stage. There are a number of indications that the stoichiometry can be as large as 30:1 before solubilization, e.g.[88,89] The concentration/activity of the corresponding bulk complex will then almost inevitably pass through a maximum before precipitation and the ST may then correspondingly pass through a minimum and cause the appearance of an ST peak. However, for a surface complex with $\gamma > 1$ such an ST peak cannot occur until the resolubilization stage, i.e. significantly above the onset of precipitation.

We start by considering the peaks that appear in the PDDA-SDS system with and without electrolyte. The dominant surface complex with electrolyte has the stoichiometry $\gamma \approx 0.5$. On the basis of the small effect of electrolyte on γ mentioned above we assume that γ is the same with and without electrolyte. The change in ST below precipitation will be sensitive to differences in binding in both cooperative and non-cooperative regions and therefore particularly to the value of ϕ_{max}, i.e. the value of the bound fraction at the changeover. The binding isotherm of the PDDA-SDS system without electrolyte was shown in Figure 7(b) and has a cooperative binding limit of $\phi_{max} = 0.6 - 0.8$ (0.8 was used to fit the data in the figure). The binding isotherm in the presence of 0.1M NaCl is shown in Figure 11 and gives a value of $\phi_{max} = 0.8$. Overall, γ is therefore slightly lower than ϕ_{max}. For a combination of high cooperativity and a narrow distribution of γ, together with $\gamma < \phi_{max}$, surface active complexes will be present at a significant bulk concentration from the onset of binding at

$\phi = 0$ to the end of cooperativity at ϕ_{max}, but they will then largely vanish. This is because once cooperative binding is complete the large majority of the bulk complexes will have a stoichiometry of at least ϕ_{max} and there will be none of the lower stoichiometry surface active species left. There will therefore be a substantial decrease in the concentration of the surface active species, with an associated upturn in the ST at $s_{total} = \phi_{max}[\mathrm{X}] + s_f^*$, where s_f^* is the free surfactant concentration at the onset of precipitation and [X] is the polymer monomer concentration. This function has already been plotted for PDDA in Figure 14, where its slope suggests a value of $\phi_{max} = 0.75$, within error of the independent estimate of ϕ_{max} from the binding curve. This result shows that the sharp rise in ST almost certainly results from a rapid decline to zero of the concentration of the main surface active species SX_2 at the cooperative binding limit. Although this change must be close to the onset of precipitation, precipitation cannot have the same effect. We also note that the precipitate is, in any case, not the complex being adsorbed.

The sharp rise in ST for PDDA-SDS with electrolyte occurs directly from the plateau region B but, in the absence of electrolyte, the rise in ST is preceded by a drop in ST characteristic of the onset of the effect of non-cooperative binding in region C following a high ST plateau in region B. In this case the loss of surface activity must therefore occur above ϕ_{max}, not below. For PDDA-SDS without electrolyte there is indeed a downward shift of about an order of magnitude in the concentration at which ϕ_{max} is reached because $1/K$ decreases by about an order of magnitude in the absence of electrolyte, which is clearly sufficient to cause ϕ_{max} to drop below γ. The decrease in ST at the changeover from B to C regions then occurs because s_{free} increases rapidly when ϕ_{max} is reached, as shown in Figure 10 and Figure 8, and this will increase the concentration of all species of complex in the bulk. However, the concentration of the surface active species can be expected to decrease as soon as the overall stoichiometry exceeds γ and this will then reverse the drop in ST. The decrease will be a complicated function of the cooperative and non-cooperative binding as well as the spread of surface activity with stoichiometry. However, the Gibbs equation

with a moderate level of adsorption will turn this maximum in the concentration of the bulk complex with stoichiometry γ into a V-shaped ST dip, as observed, which will also be sharp if there is a relatively narrow spread of stoichiometry of the surface active species.

The surface behaviour of PDDA with different chainlength surfactants is also consistent with this pattern if γ for $SC_{10}S$ and $SC_{14}S$ is assumed to have the same value of 0.5 as for SDS ($SC_{12}S$). This is to be expected if it is driven mainly by head group-segment interactions. The values of ϕ_{max} will, however, be different because they are driven by the hydrophobicity, which increases from C_{10} to C_{14}. The low concentration ST behaviour has already shown that the $SC_{10}S$ system behaves almost completely non-cooperatively, i.e. $\phi_{max} \approx 0$. In this case the only point at which the $\gamma = 0.5$ surface species are likely to be removed from the surface is when s_{total} rises to a value where almost all the complexes are saturated. When binding is weak this is only possible if there is a large excess of surfactant. Thus, the $SC_{10}S$ system requires a substantially larger s_{total} than required for nominal equivalence and a peak does indeed appear at an unusually high surfactant concentration (Figure 12). When electrolyte is added the binding curve is shifted upwards by an order of magnitude and hence this point cannot now be reached, as observed. The large drop in ϕ_{max} on going from SDS to $SC_{10}S$ should be matched by an equivalent increase for $SC_{14}S$. If, as expected, ϕ_{max} increase to ≈ 1 the binding will remain in the cooperative region up to where free surfactant dominates the ST, i.e. there will be no dip in the ST. Addition of electrolyte in this case shifts the binding curve to higher concentration and again no ST anomaly is expected, as observed (Figure 13).

It is interesting to explore how the high value of $\gamma \approx 2$ observed for the surface adsorption in PSS-C_{12}TAB systems may also generate an ST peak. The onset of precipitation is marked by the intersection of the steep decrease in ST in region C with the plateau corresponding to the onset of precipitation. This occurs close to the equivalence point as shown in Figures 14 and 9 and at a value of $s_{free} = 0.06$ mM. Above the onset of precipitation the presence of both SX and free surfactant should ensure the presence of bulk S_2X, i.e. the surface active

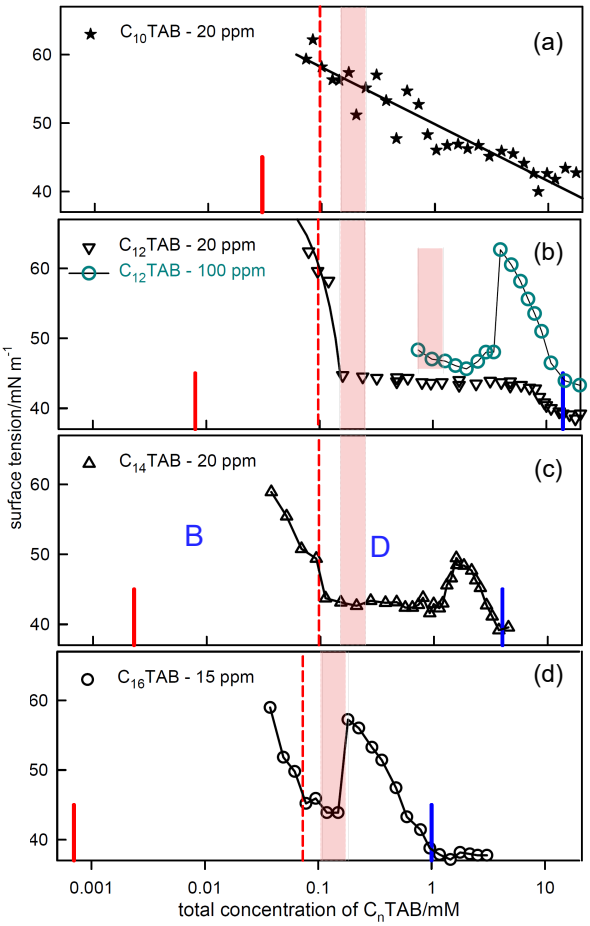

Figure 15: ST measurements for different chainlength C_nTABs with NaPSS without added electrolyte (a) C_{10}TAB, (b) C_{12}TAB, (c) C_{14}TAB and (d) C_{16}TAB.[74,76] The extra data at 100 ppm in (b) is from Varga and Campbell.[90] The equivalence points are shown as vertical dashed lines, $1/K$ is shown by short thick red lines and the CMC by blue lines, and the shaded regions indicate the composition of the surface adsorbed layer based on the value determined for PSS-C_{12}TAB by NR.

species, over a limited range of s_{total} above precipitation, and no ST peak should therefore appear over this range. The total surfactant concentration needs to be at least twice the equivalence value. Figure 15 shows the effect of surfactant chainlength on the ST behaviour of PSS-C_nTABs. The polymer concentration is fixed at 20 ppm for all except C_{16}TAB and the inset for C_{12}TAB. The polymer samples are not the same, being 18k for PSS-C_{12}TAB, and 48k for the others. The appearance of the PSS-C_{10}TAB system is quite different from the rest and equilibration for this system was particularly troublesome, which is the probable reason for the large scatter in the data.[76] The importance of the equivalence point as the

approximate definition of the onset of precipitation is clear in the three other systems and is consistent with Figure 14 and the associated explanation. The steady decline in ST for PSS-C_{10}TAB probably results from a lack of cooperative bulk binding just as observed for PDDA-C_{10}S, although the mean slope is about half that found for PDDA-C_{10}S. However, the PSS-C_{10}TAB system may be complicated by the phenomenon observed in Figure 14, in which a small fraction of surfactant appears to be incorporated into the counterion condensate. Such an effect would be expected to be enhanced for the less hydrophobic C_{10} chain, and this would then lead to a reduced Gibbs prefactor for the slope of the ST plot. However, both ST and NR measurements indicate multilayering over much of the concentration range, which further confuses both the measurement (difficulty of equilibration) and the interpretation of the PSS-C_{10}TAB results. Monteux et al. also found that the largest ellipticity in this series was exhibited by C_{10}TAB with an onset close to the stoichiometry of the optimum surface activity based on observations with 500 ppm samples.[91]

For the interpretation of the ST peaks for the remaining C_nTABs we again assume that the preferred surface stoichiometry γ depends mainly on head group-segment interactions and is therefore approximately independent of chainlength. For PSS-C_{12}TAB no ST peak was observed by Taylor et al. over polymer concentrations from 20 to 140 ppm. However, Varga and Campbell observed a peak at 100 ppm, which is shown as an extra insert in the figure. Whether or not this is a true equilibrium feature, the ST peak occurs, as do those of C_{14}TAB and C_{16}TAB, at a value of s_{total} which is consistently higher than the preferred surface stoichiometry, S_2X, as can be seen from the shaded regions in Figure 15(d). The distribution of γ values about the mean should both narrow and remain closer to the value of s_{total} as the cooperativity increases. Thus the probability of an ST peak occurring should increase strongly with chainlength, i.e. C_{16}TAB is much more likely to have an ST peak than C_{12}TAB, and the ST peak should occur at a value of s_{total} much closer to twice the equivalence point. Both these features are as observed. When binding is non-cooperative the stoichiometry of the bulk complexes has a broad distribution and hence the situation

where one particular stoichiometry can be effectively completely removed, as required for the occurrence of an ST peak, does not occur. There is therefore no ST peak for PSS-C_{10}TAB. We return to the marginal case of C_{12}TAB below.

Further insight comes from the ternary phase diagram determined for NaPSS with C_{16}TACl by Sitar et al.[88] and small angle x-ray and neutron experiments on the same system by Nause et al.[89] Although the change of counterion will change the details of the phase diagram, the overall pattern is expected to be comparable. The part of the phase diagram corresponding approximately to the concentration range from precipitation to higher surfactant concentrations in Figure 15 is the Surfactant-Polyion (S-P) mixing plane.[88] Although the measurements of Sitar et al. do not extend to the high dilution of the ST experiments, the S-P mixing plane indicates that there are just two coexisting phases at the start of region D, which are a hexagonal 1:1 phase, which contains nearly all the polymer, and a micellar phase, or monomer at higher dilution. The initial phase separation (for C_{12}TAB) signalled by the ST experiments, i.e. the onset of the ST plateau, is the formation of the hexagonal phase determined independently by Hansson and Almgren.[73] As further surfactant is added, a single phase, i.e. complete redissolution, is not reached until the ratio of surfactant to complex reaches a relatively high value, estimated from the phase diagram to be a molar ratio of at least 15.[88] This suggests that significant amounts of surfactant are gradually incorporated into the hexagonal phase, i.e. it becomes a swollen hexagonal phase with a surfactant stoichiometry higher than 1. The experiments by Nause et al. indicate that the hexagonal phase starts to form at a lower stoichiometry $S_{0.7}X$ than the 1:1 SX found by Sitar et al. (a difference between the two experiments was that Nause et al. had added electrolyte, although at the low level of 10 mM NaCl). A further difference is that the hexagonal phase gradually transforms into a cubic phase, a transformation that is complete at about $S_{1.5}X$ in 10 mM NaCl. The dependence of the phase boundary on polymer concentration as determined by ST (Figure 14) gives a value of $S_{0.9}X$, intermediate between the 1:1 of Sitar et al. and the 0.7 of Nause et al. The existence of a cubic phase reinforces the idea that the progress to

resolubilization is thermodynamically reasonably well defined. A final comment is that the well defined micellar structures identified by Nause et al. at surfactant stoichiometries below $S_{0.7}X$ are far from the kind of structures that would be surface active. Their stability may be one reason why there is no adsorption of low stoichiometry complexes.

There are some less obvious features that are consistent with the above mechanism. Thus, at the point where the bulk concentration of the preferred surface active complex starts to drop, the adsorption of this complex should also decrease. This is observed by NR particularly clearly in the cases of PDDA-SDS and PDDA-$SC_{10}S$ both without electrolyte (Figures 10 and 12). The surface excess for both of these systems at low s_{total} is much higher than for SDS on its own but, as the end of the C region is approached it drops over a range of s_{total} before again increasing and following the upward trend of the adsorption expected for SDS alone. The combination of the drop in surface excess followed by the increase results in a dip that coincides with an ST peak. A dip also occurs in PDDA-$SC_{10}S$ with electrolyte (Figure 12) but the ST peak that would then be expected is evidently suppressed by the much lower ST for $SC_{10}S$ when electrolyte is present. The dip in surface excess is weaker but still evident for 10 ppm PDDA-SDS with electrolyte though not for the 80 ppm sample (Figure 11). However, what is interesting in the latter system is the change in composition of the surface, which can be seen particularly clearly for PDDA-SDS with electrolyte in Figure 10(a). At 10 ppm the SX_2 is replaced by complex with slightly more X, suggesting that the loss of surface activity is greater when S is increased than when it is decreased. At 80 ppm, where the rise in ST is much sharper, the composition of the surface moves in the expected direction, i.e. richer in surfactant at the peak. The pattern of the ST rise, however, will clearly be highly dependent on the details of the binding isotherm and the pattern of variation of surface activity with stoichiometry. A final important observation is that NR unequivocally demonstrates the presence of polymer at the surface at most concentrations, including at the actual ST peak in the 80 ppm sample. This is consistent with the mechanism where complexes close to SX stoichiometry have reduced rather than no surface activity.

In principle, a drop in surface coverage also ought to occur before the ST peak in PSS-C_nTAB systems. Such a drop is clearly observed for C_{14}TAB where the surface excess (of surfactant) is 3.9 μmol^{-2} at the upper edge of the shaded zone in Figure 15, but then drops to 2.6 and 2.8 μmol^{-2} between this point and the onset of the ST peak, where it remains low. On the upper side of the ST peak it increases again to 3.5 μmol^{-2} and at higher concentrations it forms multilayers. There is no ST peak in the measurements of Taylor et al. on PSS-C_{12}TAB and adsorption is constant within error across the plateau. When s_{total} is approximately at or above the CMC of the free surfactant, stable multilayering occurs.[74]

Equilibration

For regions A, B and C the above description ties together binding isotherm, surface excess, surface composition and ST in the Gibbs equation using the approximation that the surface behaviour is dominated by a single complex $S_\gamma X$ and that the activity of this complex depends on s_{free}. However, while consistency with the *changes* in ST given by the Gibbs equation indicates that the surface is at equilibrium, the *absolute* value of the ST is less accessible. This is particularly the case for polymer systems where extrapolation to low concentration raises more or less intractable problems[92,93] in the determination of the absolute ST. This can arise in PE-S systems when there is a high ST at the onset of region B, as is often the case in the absence of electrolyte. Thus, if there is no adsorption in region A, there may be a negligible depression of the ST from that of the dilute polymer solution (usually approximately that of water), while the NR experiment shows a substantial surface excess. This may seem intuitively unreasonable, but a PE-S complex occupies a large surface area, so that even a small decrease of ST per monomer can provide enough free energy to overcome the opposing small loss of entropy and bring about adsorption. However, in these cases longer time measurements (8 hr) of the ST often indicate that the ST reaches much lower values than those measured at shorter times (1 hr) and the true equilibrium situation with respect to both ST and surface excess is therefore in doubt. The main potential difficulty in attaining

surface equilibration of polymers comes from polydispersity of MW and/or composition. Polydispersity leads to a mixture of components of differing surface activity and widely different molar concentration. Large MW species are generally adsorbed more strongly than low MW species but if they are only present at low concentrations they equilibrate with the surface extremely slowly. The long time ST measurements on PE-S systems generally exhibit drops in ST that are extremely slow in the absence of electrolyte and the final ST values for several of the systems so far discussed are significantly lower in region B than those obtained on the shorter timescale, e.g.[94] However, there seems to be no corresponding variation in the direct NR experiment. In direct measurements of adsorbed amounts using NR the sample is typically in place up to 3 hrs before measurements start, and some samples may be measured more than once at intervals of up to 3 hrs over an even longer period. NR is entirely non-invasive, unlike ST, and the sample is in a teflon trough in an atmosphere that is sealed for the duration of a set of experiments, so there can be no surface effects created by evaporation[95] and the surface is not disturbed during the measurement. The monolayers seen by NR in regions A, B and C normally reach their final state typically in less than 1 hr, a timescale that is in line with the expected diffusion times. However, a typical NR measurement will not be sensitive to the replacement of smaller polymers by larger ones, because it normally measures only the surfactant. NR experiments that determine the amount of polymer indirectly at the surface have a lower accuracy, and even direct measurements using deuterated polymer would find it difficult to distinguish different MWs at the surface.

An example of the discrepancy occurs for PSS-C_{12}TAB without added electrolyte. Taylor et al. (18k)[74] and Monteux et al. (42k)[18] directly observed significant adsorption in the B region, but both groups also found that the ST after about 1 hr remained constant and close to that of pure water (72 mN m^{-1}). However, Noskov et al. (70k)[94] found that the ST of a PSS-C_{12}TAB mixture took about 8 hr to reach a lower stable ST of 60 mN m^{-1}, in a region where Figure 9 indicates an ST close to that of water. For PDDA-SDS without electrolyte the

long time results of Noskov et al. (MW 100-200k)[96] show a moderate drop from water and a steady decline with increasing surfactant concentration, which is not consistent with the combination of the Gibbs equation and the highly cooperative isotherm,[71,81,82] which should lead to a long ST plateau, as observed by Penfold et al.[80](MW 200k). Despite these large discrepancies, the patterns of ST behaviour generally agree. Thus, both sets of experiments show the sharp dip in ST at region C followed by a peak in region D. For the same system with added electrolyte, Lyadinskaya et al.[97] found more rapid equilibration and the results for regions A and B show reasonable agreement with those of Staples et al.[83] There is some difference in the slope in the A region but the polymer concentration independence of the switch from A to B matches the onset of cooperative binding observed by Staples et al.

The calculation of the absolute value of the ST at the onset of a plateau B requires a knowledge of the adsorption behaviour back to much lower concentrations than the measurements. In the case when both ST and adsorption are high the calculations described above assume that no adsorption occurs below the onset of binding in the bulk solution. This assumption may well be correct for the nominal MW species. However, although adsorption is unfavourable below the onset of bulk binding, the adsorption energy *per polymer molecule* is expected to increase with MW, so that some adsorption of high MW complexes may occur at lower concentrations. The rate of formation of such complexes at the surface will be very slow because the largest polyions in the system will be present at a very low molar concentration. However, even if the adsorption is at a low level there may be a significant lowering of the ST because the Gibbs equation has a large prefactor for the dissociated complex. The *true* equilibrium ST at higher concentrations would then be that of a mixture of the bound bulk complexes with a low Gibbs prefactor with a small number of high MW species with a large Gibbs prefactor. It may even be that this cannot be attained in practice because depletion effects (of the larger MW) will increase with the MW. Thus, the short time ST measurements and the relative insensitivity of NR to the polymer may be more representative of an ideal "monodisperse" system, although the long time measurements are closer to

the true equilibrium value for the real polydisperse system.

Equilibration in region D involves the triple problem of low solubility precipitate, slow diffusion of polymer, and polydispersity of the polymer. There are two conflicting requirements. Equilibration of the bulk system of a sparingly soluble material formed by mixing requires vigorous treatment, whereas obtaining an equilibrium surface requires minimal disturbance for the actual measurement, although light disturbance of the surface ahead of the measurement may help equilibration. The formation of a precipitate will follow Ostwald's Step Rule, which is that initial nucleation forms the metastable phase closest in stability to the starting solution, which may then evolve via a sequence of intermediate metastable states to the thermodynamically most stable structure, e.g. Chung et al.[98] In PE-S systems a colloidal precipitate is a common example of an intermediate metastable state.[99] In the measurement of low solubility crystallizations, vigorous agitation is considered to be a prerequisite to ensure transformation through metastable intermediates to the final thermodynamic state.[100] The phase diagram of NaPSS-C_{16}TAB obtained by Sitar et al.,[88] and discussed above, not only used vigorous mixing conditions but also used the other key step in such measurements, which is the structural characterization of the final precipitate.[100] The achievement of surface equilibrium of a sparingly soluble solute, even without the complication of in situ formation, is also challenging and requires special procedures to maintain a saturated monolayer, as illustrated by a series of measurements by Franses et al. on the surface behaviour of long chain alkanols.[101–104] In particular, the presence of the solid phase, preferably finely divided, was found to be necessary for the determination of the ST of saturated hexadecanol[101] because of losses either to the vapour phase or to the surfaces of the solid container. Their work suggests that, provided the precipitate is more dense than the solution, any surface measurements are best done using a solid + saturated mixture that has been vigorously mixed prior to being loaded into a trough for a surface measurement.

Campbell and coworkers have followed a different route in which gentle mixing of polyelectrolyte and surfactant solutions is followed by standing, without stirring, over periods of

up to a month and sampling for external measurement by taking care "not to agitate any settled precipitate at the bottom of the flasks in order to avoid the redispersion of surface-active material".[90] Given the comment in the previous paragraph, this may lead to results where either metastable rather than full equilibrium is reached and/or surface depletion occurs because there is no solid present to maintain saturation. However, this method appears to work in the case of for PDDA-SDS in 100 mM NaCl because Varga and Campbell (VC) obtained an ST peak for 10 ppm PDDA in good agreement with that shown in Figure 10 and obtained much earlier by Staples et al., who used vigorous short time mixing. The agreement is strong evidence that full equilibration in this system occurs under both sets of conditions.[20] However, the ST peak observed by VC for 100 ppm PSS-C_{12}TAB after one month of static conditions disagrees with earlier ST results obtained using short timescale vigorous mixing[74,76,105] (Figure 15(b)). As discussed above, PSS-C_{12}TAB is intermediate between PSS-C_{14}TAB, which exhibits an ST peak with the expected pattern of dependence on polymer concentration, and PSS-C_{10}TAB, which does not exhibit an ST peak. The difference in free energy between the alternative patterns of behaviour is therefore small, making it easy to reach a metastable state. VC interpreted their turbidity data as showing that the two phase region exists only in the range of heaviest precipitation (3-10 mM), whereas phase separation is normally at the *onset* of precipitation, which occurs at a concentration an order of magnitude lower.[73,89] Turbidity may, of course, arise without a phase transition and the most reliable alternative is then to measure the phase change "via a discontinuity in a property associated with it".[100] In this case, the ST is just such a property and shows a sharp and easily measured transition[74] with the expected polymer concentration dependence (Figure 14)[74] and in agreement with independent non-ST measurements.[73,89] However, although VC measured the ST, the measurements did not extend to the equivalence point, which is close to where the onset of precipitation would be expected (Figure 10). As already discussed, Sitar et al. have shown that in both PSS-C_{12}TAB and PSS-C_{16}TAB phase separation produces a hexagonal phase, which includes more or less all of the polymer and a solution phase, the

solution phase being micellar or monomer depending on the concentration and chainlength. In PSS-C_{16}TAB Sitar et al. further showed that the hexagonal phase becomes swollen by extra surfactant before resolubilization is achieved. It is evidently the onset of sedimenting swollen material that is being identified as the onset of precipitation by VC.

The explanation of the ST peak given above for the PSS-C_nTAB series was that it results from the removal of the surface active species S_2X from solution as the overall stoichiometry increases past the S_2X composition. The trend in the series PSS-C_nTAB indicates that the cooperativity of binding of surfactant to the swollen hexagonal phase is not quite sufficient to reduce bulk [S_2X] sufficiently to cause a peak in the ST of PSS-C_{12}TAB. The metastability of the ST peak for PSS-C_{12}TAB is consistent with a trend from true equilibrium ST peaks for PSS-C_{16}TAB and PSS-C_{14}TAB through a metastable ST peak for C_{12}TAB to no ST peaks for C_{10}TAB. A further indication of the metastability in the plateau region between the onset of precipitation and the drop in ST at the end of resolubilization was reported by Taylor et al. Stable multilayering in PSS-C_{12}TAB and PSS-C_{14}TAB is observed at concentrations above this plateau. However, Taylor et al. noted that on the plateau there were two instances of time dependent multilayering,[74] which are consistent with metastability in this region, although no ST peak was observed. The combination of the absence of solid phase in VC's measurement and the absence of an ST peak in any of the *four* samples at different PSS concentrations measured by Taylor et al. suggests that no ST peak is the equilibrium behaviour. However, the more interesting result is that the erratic ST behaviour of PSS-C_{12}TAB is clearly part of a systematic trend, which leads to the PSS-C_{14}TAB system exhibiting both an ST peak and multilayers, i.e. they are not mutually exclusive, as had been suggested by the original empirical division into Type 1 and Type 2 behaviour.

Attempts have been made to explain the equilibrium ST behaviour of PE-S mixtures by dividing the complex into two states in order to model the ST. Thus, Ritacco and Busch divided the PE-S into free surfactant and PE-S complex[106] based on an earlier division of a single surfactant with two possible states of adsorption by Fainerman et al.[107] The division

used by Fainerman et al. is equivalent to, for example, modelling the ST of a surface active weak acid in terms of an interacting mixture of dissociated and undissociated species, which is a valid alternative to treating the system as a single component in dissociative equilibrium, which is what has been done in the present paper. Either procedure is valid in the case of a surface active weak acid because it is thermodynamically a single component. This is not the case for a PE-S mixture, where the choice reduces to the most convenient or accurate approximations. Here, we have made use of the characteristic properties of the binding isotherm to treat the PE-S complex as a single entity. Our previous models of PE-S systems have effectively been two state models. Thus, Bell et al. used a mass action model based on a division into a surface active complex and a non-surface active complex. Bahramian et al. used the Gibbs equation but modelled the phase separation region in terms of composite activities determined from the limiting activities of the components and the concentration. Here, we have essentially extended the Bahramian approach but have used the bulk binding isotherm to characterize the bulk activity variation of the PE-S complex as a single entity.

Conclusions

In a previous paper we established some preliminary links of the binding isotherms for the formation of PE-S complexes with their surface behaviour at the air-water interface. These links were incomplete and relied significantly on qualitative descriptions of model structures of the adsorbed aggregates and their related bulk complexes. Here we have extended those links by successfully combining thermodynamic information from binding curves and experimental measurements of surface excess and composition at the air-water interface in the Gibbs equation. This explains the equilibrium surface tension behaviour for two groups of PE-S complexes, independent of any detail of the structure of the complexes. The surface behaviour can be divided into four surfactant concentration regions, which we label A, B, C and D, and each can be fitted semi-quantitatively by the Gibbs equation. The analysis is based on the change between cooperative and non-cooperative binding in the bulk solu-

tion and demonstrates the importance of having measurements of the surface composition. The implication of being able to account for the ST behaviour with the Gibbs equation is that both bulk and surface of the solution are adequately equilibrated. This might seem surprising given the many indications that the precipitate itself is not at equilibrium, but precipitation, although a useful marker of an important part of the phase diagram, does not play a major role in either the Gibbs equation or the equilibrium ST behaviour. In a system of low solubility, the free surfactant, which dominates the surfactant activity in a heterogeneous system, may reach an equilibrium value even if only a small fraction of the precipitate is in its equilibrium form.

The analysis shows that the empirical distinction between Type 1 and Type 2 systems made in the Introduction is only approximate. Thus, the empirical observation was that if the initial drop in ST is dependent on the polymer concentration there should be no peak in the ST at higher concentrations (Type 1 behaviour). However, it is now clear that these two phenomena are independent of one another. The initial ST drop may occur either if adsorption occurs before there is any bulk binding or when the bulk binding changes from cooperative to non-cooperative. Since the latter occurs only when the system reaches a certain bound fraction, it is directly proportional to the polymer concentration. The primary cause of an ST peak is that there is a strongly preferred stoichiometry of the adsorbed species and adsorption becomes significant when the concentration of the corresponding bulk complex reaches a sufficient concentration. Depending on the pattern of complex formation the addition of further surfactant may convert this complex into one of higher stoichiometry and hence its concentration drops. If this drop is large, the ST may increase more or less sharply. Since the addition of even more surfactant will eventually lower the ST, the result may be an ST peak but this is not related to the dependence of the ST on polymer concentration. The final correlation was that an ST peak indicates that there will be no multilayer formation. Whatever the mechanism of multilayering,[11] it requires a combination of strong surface activity and a high enough concentration to favour aggregation. Since the

occurrence of an ST peak is associated with removal of the most surface active complex into a bulk phase, the presence of an ST peak would indeed seem to prevent adsorption, including multilayers. However, this is not a completely reliable indicator. Thus, PSS-C_{14}TAB has what is probably an equilibrium ST peak and forms multilayers. However, as demonstrated by the metastability of the ST peak in PSS-C_{12}TAB and the evolution of the pattern of ST peak formation in the PSS-C_nTAB series, the crossover from ST peak to no ST peak can be sufficiently delicate that it may be perturbed by changes in concentration or composition, which then allows both features to occur. This is, however, expected to be highly unusual.

Supporting Information

A diagram (Figure S1) of the experimentally determined variation of axial charge density and counterion condensation for NaPSS as a function of molecular weight is shown. The data from this is used in the analysis of the ST of NaPSS in the main body of the paper.

References

(1) Goddard, E. D. Polymer-surfactant interaction, part II: Polymer and surfactant of opposite charge. *Colloids Surf.* **1986**, *19*, 301–329.

(2) Goddard, E. D. Polymer-surfactant interaction: Interfacial aspects. *J. Colloid Interface Sci.* **2002**, *256*, 228–235.

(3) Thompson, L. The role of oil detachment mechanisms in determining optimum detergency conditions. *J. Colloid Interface Sci.* **1994**, *163*, 61–73.

(4) Penfold, J.; Thomas, R. K.; Taylor, D. J. F. Polyelectrolyte-surfactant mixtures at the air–solution interface. *Current Opinion Colloid Interface Sci.* **2006**, *11*, 337–344.

(5) Taylor, D. J. F.; Thomas, R. K.; Penfold, J. Polymer-surfactant interactions at the air-water interface. *Adv. Colloid Interface Sci.* **2007**, *132*, 69–110.

(6) Langevin, D. Complexation of oppositely charged polyelectrolytes and surfactants in aqueous solutions. A review. *Adv. Colloid Interface Sci.* **2009**, *147—148*, 170–177.

(7) Bain, C. D.; Claesson, P. M.; Langevin, D.; Meszaros, R.; Nylander, T.; Stubenrauch, C.; Titmuss, S.; von Klitzing, R. Complexes of surfactants with oppositely charged polymers at surfaces and in bulk. *Adv. Colloid Interface Sci.* **2010**, *55*, 32–49.

(8) Llamas, S.; Guzmana, E.; Ortega, F.; Baghdadli, N.; Cazeneuve, C.; Rubio, R. G.; Luengo, G. S. Adsorption of polyelectrolytes and polyelectrolytes-surfactant mixtures at surfaces: a physico-chemical approach to a cosmetic challenge. *Adv. Colloid Interface Sci.* **2015**, *222*, 461–487.

(9) Guzman, E.; Llamas, S.; Maestro, A.; Fernandez-Pena, L.; Akanno, A.; Miller, R.; Ortega, F.; Rubio, R. Polymer-surfactant systems in bulk and at fluid interfaces. *Adv. Colloid Interface Sci.* **2016**, *233*, 38–64.

(10) Braun, L.; Uhlig, M.; von Klitzing, R.; Campbell, R. A. Polymers and surfactants at fluid interfaces studied with specular neutron reflectometry. *Adv. Colloid Interface Sci.* **2017**, *247*, 130–148.

(11) Li, P. X.; J., P.; Thomas, R. K.; Xu, H. Multilayers formed by polyelectrolyte-surfactant and related mixtures at the air-water interface. *Adv. Colloid Interface Sci.* **2019**, *269*, 43–86.

(12) Thomas, R. K.; Penfold, J. Multilayering of surfactant systems at the air-dilute aqueous solution interface. *Langmuir* **2015**, *31*, 7440–7456.

(13) Bell, C. G.; Breward, C. J. W.; Howell, P. D.; Penfold, J.; Thomas, R. K. Macroscopic modeling of the surface tension of polymer-surfactant systems. *Langmuir* **2007**, *23*, 6042–6052.

(14) Bell, C. G.; Breward, C. J. W.; Howell, P. D.; Penfold, J.; Thomas, R. K. A theoretical analysis of the surface tension profiles of strongly interacting polymer–surfactant systems. *J. Colloid Interface Sci.* **2010**, *350*, 48–493.

(15) Bahramian, A.; Thomas, R. K.; Penfold, J. The adsorption behavior of ionic surfactants and their mixtures with nonionic polymers and with polyelectrolytes of opposite charge at the air-water interface. *J. Phys. Chem. B* **2014**, *118*, 2769–2783.

(16) Kogej, K. Association and structure formation in oppositely charged polyelectrolyte-surfactant mixtures. *Adv. Colloid Interface Sci.* **2010**, *158*, 68–83.

(17) Li, G. B.; Ma, H. M.; Hao, J. C. Surfactant ion-selective electrodes: A promising approach to the study of the aggregation of ionic surfactants in solution. *Soft Matter* **2012**, *8*, 896–909.

(18) Monteux, C.; Williams, C. E.; Meunier, J.; Anthony, O.; Bergeron, V. Adsorption of oppositely charged polyelectrolyte-surfactant complexes at the air-water interface: formation of interfacial gels. *Langmuir* **2004**, *20*, 57–63.

(19) Li, D. C.; Wagner, N. J. Universal binding behavior for ionic alkyl surfactants with oppositely charged polyelectrolytes. *J. Am. Chem. Soc.* **2014**, *135*, 17547–17555.

(20) Thomas, R. K.; Penfold, J. Thermodynamics of the air-water interface of mixtures of surfactants with polyelectrolytes, oligoelectrolytes and multivalent metal electrolytes. *J. Phys. Chem. B* **2018**, *122*, 12411–12427.

(21) Oosawa, F. *Polyelectrolytes*; Marcel Dekker, 1971.

(22) Manning, G. The molecular theory of polyelectrolyte solutions with applications to the electrostatic properties of polynucleotides. *Quart. Rev. Biophysics* **1978**, *11*, 179–246.

(23) Muthukumar, M. Theory of counter-ion condensation on flexible polyelectrolytes: adsorption mechanism. *J. Chem. Phys.* **2004**, *120*, 9343–9350.

(24) Netz, R. R.; Andelman, D. Neutral and charged polymers at interfaces. *Phys. Reports* **2003**, *380*, 1–95.

(25) Manning, G. S. Limiting laws and counterion condensation in polyelectrolyte solutions I. Colligative properties. *J. Chem. Phys.* **1969**, *51*, 924–933.

(26) Ise, N.; Okubo, T. Thermodynamic and kinetic properties of polyelectrolyte solutions. A unified interpretation in terms of Manning's theory. *Macromolecules* **1978**, *11*, 439–447.

(27) Prigogine, I.; Defay, R.; Bellemans, A.; Everett, D. H. *Surface tension and adsorption, Chapter XXI, Sections 8 and 9*; Longman: London, 1966.

(28) Manning, G. In *Polyelectrolytes*; Selegny, E., Ed.; D.Reidel: Dordrecht, 1974; pp 9–38.

(29) von Klitzing, R.; Kolaric, B.; Jaeger, W.; Brandt, A. Structuring of poly(dimethyldiallylammonium chloride) chains in aqueous media: a comparison between bulk and free-standing film measurements. *Phys. Chem. Chem.Phys.* **2002**, *4*, 1907–1914.

(30) Marcelo, G.; Tarazona, M.; Saiz, E. Solution properties of poly(diallyl dimethyl ammonium chloride) (PDDA). *Polymer* **2004**, *45*, 1321–1330.

(31) Marcelo, G.; Tarazona, M.; Saiz, E. Solution properties of poly(diallyl dimethyl ammonium chloride) (PDDA). *Polymer* **2005**, *46*, 2584–2594.

(32) Ikeda, S. The Gibbs adsorption isotherm for aqueous electrolyte solutions. *Adv. Colloid Interface Sci.* **1982**, *18*, 93–130.

(33) Nishida, K.; Kaji, K.; Kanaya, T. Improved phase diagram of polyelectrolyte solutions. *J. Chem. Phys.* **2001**, *115*, 8217–8220.

(34) Muthukumar, M. Electrostatic correlations in polyelectrolyte solutions. *Polymer Sci. A* **2016**, *58*, 852–863.

(35) Noskov, B. A.; Nuzhnov, S. N.; Loglio, G.; Miller, R. Dynamic surface properties of sodium poly(styrenesulfonate) solutions. *Macromolecules* **2004**, *37*, 2519–2526.

(36) Caminati, G.; Gabrielli, G. Polystyrene sulfonate adsorption at water-graphon and water-air interfaces. *Colloids Surfaces A* **1993**, *70*, 1–14.

(37) Kanaya, T.; Kaji, K.; Kitamaru, R.; Higgins, J. S.; Farago, B. Dynamics of polyelectrolyte solutions by neutron spin echo: molecular weight dependence. *Macromolecules* **1989**, *22*, 1356–1359.

(38) An, S. W.; Thomas, R. K.; Forder, C.; Billingham, N. C.; Armes, S. P.; Penfold, J. Behavior of nonionic water soluble homopolymers at the air-water interface: neutron reflectivity and surface tension results for poly(vinyl methyl ether). *Langmuir* **2002**, *18*, 5064–5073.

(39) Böhme, U.; Scheler, U. Counterion condensation and effective charge of poly(styrenesulfonate). *Adv. Colloid Interface Sci.* **2010**, *158*, 63–67.

(40) Huber, K.; Scheler, U. New experiments for the quantification of counterion condensation. *Current Opinion Colloid Interface Sci.* **2012**, *17*, 64–73.

(41) Li, P. X.; Li, Z. X.; Shen, H. H.; Thomas, R. K.; Penfold, J.; Lu, J. R. Application of the Gibbs equation to the adsorption of nonionic surfactants and polymers at the air-water interface: comparison with surface excesses determined directly using neutron reflectivity. *Langmuir* **2013**, *29*, 9335–9351.

(42) Ise, N. The mean activity of coefficient of polyelectrolytes and its related properties. *Adv. Polymer Sci.* **1971**, *7*, 536–593.

(43) Dolar, D.; Leskovesk, H. The mean activity coefficient of polystyrenesulphonic acid. *Makromolekulare Chemie* **1968**, *118*, 60–65.

(44) Dolar, D. In *Polyelectrolytes*; Selegny, E., Ed.; D.Reidel: Dordrecht, 1974; pp 97–113.

(45) Ise, N.; Okubo, T. Mean activity coefficient of polyelectrolytes. VIII. Osmotic and activity coefficients of polystyrenesulfonates of various gegenions. *J. Phys Chem.* **1968**, *72*, 1361–1366.

(46) Okubo, T. Surface tension of synthetic polyelectrolyte solutions at the air-water interface. *J. Colloid Interface Sci.* **1988**, *125*, 386–398.

(47) Natsheh, M. A. F.; Ayyad, A. Temperature induced adsorption of sodium poly(styrenesulfonate) to the water air interface. *Materials Lett.* **2015**, *160*, 378–380.

(48) Yim, H.; Kent, M. S.; Matheson, A.; Stevens, D. M.; Ivkov, R.; Satija, S.; Majewski, J.; Smith, G. S. Adsorption of poly(styrenesulfonate) to the air surface of water by neutron and X-ray reflectivity and surface tension measurements: polymer concentration dependence. *Macromolecules* **2002**, *35*, 9737–9747.

(49) Kwak, J. Mean activity coefficients for the simple electrolyte in aqueous mixtures of polyelectrolyte and simple electrolyte. The system sodium polystyrenesulfonate-sodium chloride. *J. Phys. Chem.* **1973**, *77*, 2790–2793.

(50) Kwak, J.; O'Brien, M. C.; MacLean, D. A. Mean activity coefficients for the simple electrolyte in aqueous mixtures of polyelectrolyte and simple electrolyte. The systems potassium chloride-potassium poly(styrenesulfonate), magnesium chloride-magnesium poly(styrenesulfonate), and calcium chloride-calcium poly(styrenesulfonate. *J. Phys. Chem.* **1975**, *79*, 2381–2386.

(51) Yim, H.; Kent, M.; Matheson, A.; Ivkov, R.; Satija, S.; Majewski, J.; Smith, G. S. Adsorption of poly(styrenesulfonate) to the air surface of water by neutron reflectivity. *Macromolecules* **2000**, *33*, 6126–6133.

(52) Xu, G. F.; Yang, J. F.; Zhao, J. Molecular weight dependence of chain conformation of strong polyelectrolytes. *J. Chem. Phys.* **2018**, *149*, 163329.

(53) Frommer, M. A.; Miller, I. R. Adsorption of DNA at the air-water interface. *J. Phys. Chem.* **1968**, *72*, 2862–2866.

(54) Satake, I.; Yang, J. T. Interaction of sodium decyl sulfate with poly(L-ornithine) and poly(L-lysine) in aqueous solution. *Biopolymers* **1976**, *15*, 2263–2275.

(55) Hansson, P. Interaction between polyelectrolyte gels and surfactants of opposite charge. *Current Opinion in Colloid and Interface Science* **2006**, *11*, 351–362.

(56) Bracic, M.; Hansson, P.; Lourdes, P.; Zemljicc, L. F.; Kogej, K. Interaction of sodium hyaluronate with a biocompatible cationic surfactant from lysine: a binding study. *Langmuir* **2015**, *31*, 12043–12053.

(57) Lapitsky, Y.; Parikh, M.; Kaler, E. W. Calorimetric determination of surfactant-polyelectrolyte binding isotherms. *J. Phys. Chem. B* **2007**, *111*, 8379–8387.

(58) Malovikova, A.; Hayakawa, K.; Kwak, J. C. T. Surfactant-polyelectrolyte interactions. 4. Surfactant chain length dependence of the binding of alkylpyridinium cations to dextran sulfate. *J. Phys. Chem.* **1984**, *88*, 1930–1933.

(59) Hayakawa, K.; Santerre, J. P.; Kwak, J. C. T. The binding of cationic surfactants by DNA. *Biophys. Chem.* **1983**, *17*, 175–181.

(60) Hayakawa, K.; Murata, H.; Satake, I. Conformational change of poly(L-lysine) and poly(L-ornithine) and cooperative binding of sodium alkanesulfonate surfactants with different chain length. *Colloid Polym. Sci.* **1990**, *268*, 1044–1051.

(61) Konop, A. J.; Colby, R. H. Role of condensed counterions in the thermodynamics of surfactant micelle formation with and without oppositely charged polyelectrolytes. *Langmuir* **1999**, *15*, 58–65.

(62) van Os, N. M.; Haak, J. R.; Rupert, L. A. M. *Physico-chemical properties of selected anionic, cationic and nonionic surfactants*; Elsevier: Amsterdam, 1993.

(63) Hansson, P. Self-assembly of ionic surfactants in polyelectrolyte solutions: a model for mixtures of opposite charge. *Langmuir* **2001**, *17*, 4167–4180.

(64) Hansson, P.; Almgren, M. Interaction of CnTAB with sodium (carboxymethyl)cellulose: effect of polyion linear charge density on binding isotherms and surfactant aggregation number. *J. Phys. Chem.* **1996**, *100*, 9038–9046.

(65) Hayakawa, K.; Santerre, J. P.; Kwak, J. C. T. Study of surfactant-polyelectrolyte interactions. Binding of dodecyl- and tetradecyl-trimethylammonium bromide by some carboxylic polyelectrolytes. *Macromolecules* **1983**, *16*, 1642–1645.

(66) Delville, A. Binding of surfactant cations to DNA. A dual analysis considering ionic condensation and site binding. *Chem. Phys. Lett.* **1985**, *118*, 617–621.

(67) Nishio, T.; Shimizu, T.; Kwak, J. C. T.; Minakata, A. The cooperative binding of large ligands to a one-dimensional lattice: the steric hindrance effect. *Biophys. Chem.* **2003**, *104*, 501–508.

(68) Nishio, T.; Shimizu, T. Model analysis of surfactant-polymer interaction as cooperative ligand binding to linear lattice. *Biophys. Chem.* **2005**, *117*, 19–25.

(69) Nishio, T.; Shimizu, T.; Yoshida, S.; Minakata, A. A model study of cooperative binding of ionic surfactants to oppositely charged flexible polyions. *Condensed Matter Phys.* **2014**, *17*, 1–11.

(70) Hayakawa, K.; Kwak, J. C. T. Surfactant-polyelectrolyte interactions. 1. Binding of dodecyltrimethylammonium ions by sodium dextran sulfate and sodium poly(styrenesulfonate) in aqueous solution in the presence of sodium chloride. *J. Phys. Chem.* **1982**, *86*, 3866–3870.

(71) Lee, J.; Moroi, Y. Investigation of the interaction between sodium dodecyl sulfate and cationic polymers. *Langmuir* **2004**, *20*, 4376–4379.

(72) Shirahama, K.; Yuasa, H.; Sugimoto, S. Binding of sodium decyl sulfate to a cationic polymer. *Bull. Chem. Soc. Jap.* **1981**, *54*, 375–377.

(73) Hansson, P.; Almgren, M. Interaction of alkyltrimethylammonium surfactants with polyacrylate and poly(styrenesulfonate) in aqueous solution: phase behavior and surfactant aggregation numbers. *Langmuir* **1994**, *10*, 2115–2124.

(74) Taylor, D. J. F.; Thomas, R. K.; Penfold, J. The adsorption of oppositely charged polyelectrolyte-surfactant mixtures: Neutron reflection from dodecyl trimethylammonium bromide and sodium poly(styrene sulfonate) at the air-water interface. *Langmuir* **2002**, *18*, 4748–4757.

(75) Taylor, D. J. F.; Thomas, R. K.; Hines, J. D.; Humphreys, K.; Penfold, J. The adsorption of oppositely charged polyelectrolyte-surfactant mixtures at the air-water interface: Neutron reflection from dodecyl trimethylammonium bromide-sodium poly(styrene sulfonate) and sodium dodecyl sulfate-poly(vinyl pyridinium chloride. *Langmuir* **2002**, *18*, 9783–9791.

(76) Taylor, D. J. F.; Thomas, R. K.; Li, P. X.; Penfold, J. Adsorption of oppositely charged polyelectrolyte-surfactant mixtures: neutron reflection from alkyl trimethylammonium bromides and sodium poly(styrenesulfonate) at the air-water interface: the effect of surfactant chain length. *Langmuir* **2003**, *19*, 3712–3719.

(77) Lee, Y. L.; Dudek, A.; Ke, T. N.; Hsiao, F. W.; Chang, C. H. Mixed polyelectrolyte surfactant Langmuir monolayers at the air-water interface. *Macromolecules* **2008**, *41*, 5845–5853.

(78) Campbell, R. A.; Tummino, A.; Noskov, B. A.; Varga, I. Polyelectrolyte-surfactant films spread from neutral aggregates. *Soft Matter* **2016**, *24*, 5304–5312.

(79) Buckingham, J. H.; Lucassen, J.; Hollway, F. Surface properties of mixed solutions of

poly-L-lysine and sodium dodecyl sulfate I: equilibrium surface properties. *J. Colloid Interface Sci.* **1978**, *67*, 423–431.

(80) Penfold, J.; Tucker, I. M.; Thomas, R. K.; Taylor, D. J. F.; Zhang, X. L.; Bell, C.; Breward, C.; Howell, P. The interaction between sodium alkyl sulfate surfactants and the oppositely charged polyelectrolyte, poly(dimethyldiallylammonium chloride), at the air-water interface: The role of alkyl chain length and electrolyte and comparison with theoretical predictions. *Langmuir* **2007**, *23*, 3128–3136.

(81) Lee, J. N.; Moroi, Y. Binding of sodium dodecyl sulfate to a cationic polymer of high charge density. *Bull. Chem. Soc. Japan* **2003**, *76*, 2099–2102.

(82) Lee, J.; Moroi, Y. Solubilization of n-alkylbenzenes in aggregates of sodium dodecyl sulfate and a cationic polymer of high charge density (II). *Langmuir* **2004**, *20*, 6116–6119.

(83) Staples, E.; Tucker, I.; Penfold, J.; Warren, N.; Thomas, R. K.; Taylor, D. J. F. Organization of polymer-surfactant mixtures at the air-water interface: sodium dodecyl sulfate and poly(dimethyldiallylammonium chloride). *Langmuir* **2002**, *18*, 5147–5153.

(84) Xu, H.; Li, P. X.; Ma, K.; Thomas, R. K.; Penfold, J.; Lu, J. R. Limitations in the application of the Gibbs equation to anionic surfactants at the air-water surface: sodium dodecylsulfate and sodium dodecylmonooxyethylenesulfate above and below the CMC. *Langmuir* **2013**, *29*, 9324–9334.

(85) Nizri, G.; Lagerge, S.; Kamyshny, A.; Major, D. T.; Magdassi, S. Binding mechanism of sodium dodecyl sulfate to poly(diallyldimethylammonium chloride). *J. Colloid Interface Sci.* **2008**, *320*, 74–81.

(86) Liley, J. R.; Thomas, R. K.; Penfold, J.; Tucker, I. M.; Petkov, J. T.; Stevenson, P. S.; Banat, I. M.; Marchant, R.; Rudden, M.; Webster, J. R. P. Adsorption at the air-water

interface in biosurfactant-surfactant mixtures: quantitative analysis of adsorption in a five-component mixture. *Langmuir* **2017**, *33*, 13027–13039.

(87) Penfold, J.; Thomas, R. K. Recent developments and applications of the thermodynamics of surfactant mixing. *Molecular Physics* **2019**, *117*, 3376–3388.

(88) Sitar, S.; Goderis, B.; Hansson, P.; Kogej, K. Phase diagram and structures in mixtures of poly(styrenesulfonate anion) and alkyltrimethylammonium cations in water: significance of specific hydrophobic interaction. *J. Phys. Chem. B* **2012**, *116*, 4634–4645.

(89) Nause, R. G.; Hoagland, D. A.; Strey, H. H. Structural evolution of complexes of poly(styrenesulfonate) and cetyltrimethylammonium chloride. *Macromolecules* **2008**, *41*, 4012–4019.

(90) Varga, I.; Campbell, R. A. General physical description of the behavior of oppositely charged polyelectrolyte-surfactant mixtures at the air-water interface. *Langmuir* **2017**, *33*, 5915–5924.

(91) Monteux, C.; Williams, C. E.; Bergeron, V. Interfacial microgels formed by oppositely charged polyelectrolytes and surfactants. Part 2. Influence of surfactant chain length and surfactant-polymer ratio. *Langmuir* **2004**, *20*, 5367–5374.

(92) Linse, P.; Hatton, T. A. Mean-field lattice calculations of ethylene oxide and propylene oxide containing homopolymers and triblock copolymers at the air-water interface. *Langmuir* **1997**, *13*, 4066–4078.

(93) Vieira, J. B.; Thomas, R. K.; Li, Z. X. Adsorption of triblock copolymers of ethylene oxide and propylene oxide at the air/water interface: the surface excess. *J. Phys. Chem. B* **2002**, *106*, 5400–5407.

(94) Noskov, B. A.; Loglio, G.; Miller, R. Dilational viscoelasticity of polyelectolyte-surfactant adsorption films at the air-water interface: dodecyltrimethylammonium bromide and sodium poly(styrenesulfonate). *J. Phys. Chem. B* **2004**, *108*, 18615–18622.

(95) Aberg, C.; Sparr, E.; Edler, K. J.; Wennerström, H. Non-equilibrium phase transformations at the air-liquid interface. *Langmuir* **2009**, *25*, 12177–12184.

(96) Noskov, B. A.; Grigoriev, D. O.; Lin, S. Y.; Loglio, G.; Miller, R. Dynamic surface properties of polyelectrolyte-surfactant adsorption films at the air-water Interface: poly(diallyldimethylammonium chloride) and sodium dodecylsulfate. *Langmuir* **2007**, *23*, 9641–9651.

(97) Lyadinskaya, V. V.; Bykov, A. G.; Campbell, R. A.; Varga, I.; Lin, S. G.; Loglio, G.; Miller, R.; Noskov, B. A. Dynamic surface elasticity of mixed poly(diallyldimethylammoniumchloride)-sodium dodecyl sulfate-NaCl solutions. *Colloids Surfaces A* **2014**, *460*, 3–10.

(98) Chung, S.; Kim, Y. M.; Kim, J. G.; Kim, Y. J. Multiphase transformation and Ostwald's rule of stages during crystallization of a metal phosphate. *Nature Physics* **2009**, *5*, 68–73.

(99) Meszaros, R.; Thompson, L.; Bos, M.; Varga, I.; Gilanyi, T. Interaction of sodium dodecyl sulfate with polyethyleneimine: surfactant-induced polymer solution colloid dispersion transition. *Langmuir* **2003**, *19*, 609–615.

(100) Konigsberger, E. Editorial, guidelines for the measurement of solid-liquid solubility data at atmospheric pressure. *J. Chem. Eng. Data* **2019**, *64*, 381–385.

(101) Park, S. Y.; Chang, C. H.; Ahn, D. J.; Franses, E. I. Dynamic surface tension behavior of hexadecanol spread and adsorbed monolayers. **1993**, *9*, 3640–3648.

(102) Park, S. Y.; Francis, E. I. Hexadecanol microstructures of crystallites in aqueous dispersions and of Langmuir-Blodgett monolayers. *Langmuir* **1995**, *11*, 2187–2194.

(103) Myrick, S. H.; Franses, E. I. Effect of chain length on equilibrium and dynamic surface tension of spread monolayers of aqueous alcohols. *Colloids Surfaces A* **1998**, *143*, 503–515.

(104) Myrick, S. H.; Franses, E. I. Effect of dispersed tetradecanol particles or droplets on the dynamic surface tension of aqueous tetradecanol systems. *Langmuir* **1999**, *15*, 1556–1561.

(105) Monteux, C.; Llauro, M.; Baigl, D.; Williams, C. E.; Anthony, O.; Bergeron, V. Interfacial microgels formed by oppositely charged polyelectrolytes and surfactants. 1. Influence of polyelectrolyte molecular weight. *Langmuir* **2004**, *20*, 5358–5366.

(106) Ritacco, H. A.; Busch, J. Dynamic surface tension of polyelectrolyte/surfactant systems with opposite charges: two states for the surfactant at the interface. *Langmuir* **2004**, *20*, 3648–3656.

(107) Fainerman, V. B.; Miller, R.; Wustneck, R.; Makievski, A. V. Adsorption isotherm and surface tension equation for a surfactant with changing partial molar area. 1. Ideal surface layer. *J. Phys. Chem.* **1996**, *100*, 7669–7675.

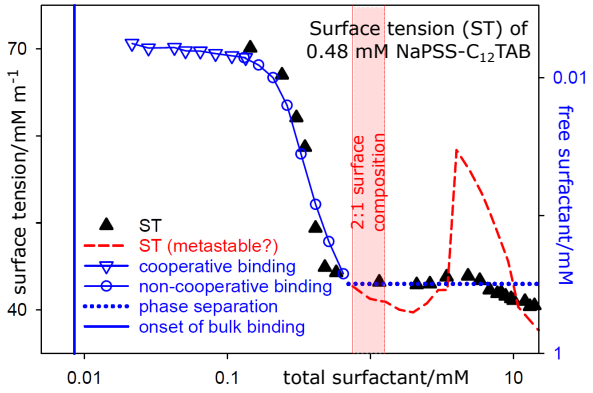
Surface tension (ST) of
0.48 mM NaPSS-C12TAB
70
40
surface tension/mM m-1
0.01
1
free surfactant/mM
2:1 surface composition
ST
ST (metastable?)
cooperative binding
non-cooperative binding
phase separation
onset of bulk binding
0.01
0.1
total surfactant/mM
10

TOC Graphic